Supporting information

NIR-II Emissive Donor-Acceptor-Donor Fluorophores for Dual Fluorescence Bioimaging and Photothermal Therapy Applications

Nicholas E. Sparks,[a] Cameron Smith,[c] Terrence Stahl,[a] Dhanush L. Amarasekara,[d] Christine Hamadani,[c] Ethan Lambert,[c] Sheng Wei Tang,[a] Anuja Kulkarni,[a] Blaine M. Derbigny,[a] Gaya Dasanayake,[c] George Taylor,[c] Maryam Ghazala,[a] Nathan I. Hammer,[c] Alexander Y. Sokolov,[a] Nicholas C. Fitzkee,[d] Eden E. L. Tanner,[c] Davita L. Watkins [a,b]*

a. Department of Chemistry and Biochemistry, The Ohio State University, Columbus, Ohio 43210, United States
b. William G. Lowrie Department of Chemical and Biomolecular Engineering, The Ohio State University, 151 W Woodruff Ave., Columbus, OH 43210, USA
c. Department of Chemistry and Biochemistry, University of Mississippi University, Oxford, MS, United States
d. Department of Chemistry, Mississippi State University, Mississippi State, MS 39762.

Corresponding author: watkins.891@osu.edu

Contents

General Summary:

All materials and reagents were purchased from commercial sources and were used without further modification unless noted otherwise. Anhydrous solvents were obtained from a Glass Contour solvent purification system (Irvine, CA, USA). Thin-layer chromatography (TLC) was performed using SiO_2-60 F254 aluminum-backed plates with visualization by ultraviolet (UV) light while flash column chromatography was performed using a Purasil SiO_2-60, 230-400 mesh from Whatman. ^{1}H and ^{13}C NMR were recorded using a Bruker Avance 400 MHz spectrometer and were recorded using solvent as an internal standard ($CDCl_3$ at 7.26 ppm). Mass spectrometry of the target compounds (0.1 mg/mL) was performed on a Bruker (Milton, ON, Canada) Elute SP HPLC with Bruker Impact II QqTOF Mass Spectrometer under electrospray ionization (ESI) conditions. Electron paramagnetic resonance (EPR) spectroscopy was performed with a Bruker (Milton, ON, Canada) Magnettech ESR5000 spectrometer with 1 mM solution ($CDCl_3$) of fluorophore. Quantification of spin states was calculated using Cu(II)$(OTf)_2$ as a reference in 1 mM THF.

Absorption and emission calculations were performed for **DMA-TTDT$_2$**, **Morp-TTDT$_2$**, and **Pip-TTDT$_2$** fluorophores, where hexyl groups on the thiophene spacers were replaced with methyl groups. The S_0 and S_1 geometries of the compounds were optimized using the CAM-B3LYP density functional with the cc-pVDZ basis set.[1–3] The calculations were carried out using an unrestricted reference wavefunction. The stability of reference wavefunction was checked using a stability analysis. Time-dependent density functional theory (TDDFT) was used to perform all excited state calculations.[4] The TDDFT calculations employed the CAM-B3LYP functional, and a modified basis set where all heteroatoms had additional diffuse basis functions (aug-cc-pvdz).[2,3,5] In addition, the solvent effects were described using a polarizable continuum model (PCM) with chloroform as a solvent.[6] For each electronic transition in TDDFT, we calculated natural transition orbitals (NTOs), which were used to quantify the orbital contributions from the amine donor and thiophene spacers.[7] Finally, natural bond orbital calculations were performed to obtain the atomic charge for all nitrogen atoms.[8] All calculations utilized the Ohio Supercomputer Center and the Q-chem quantum chemistry package.[9,10]

Absorption measurements were carried out on a Varian Cary-500 spectrometer (Dorval, OC, Canada) in $CHCl_3$. A 1 kHz regeneratively amplified Ti:Sapphire laser (Coherent Astrella, Santa Clara, California) with a 7 W, 100 fs output pulse centered at 800 nm output is split with an 85-15 beam splitter to generate pump and probe beams. To generate the pump, the reflected portion of the 800 nm output is directed into a commercial optical parametric amplifier (OPerA Solo, Vilnius, Lithuania), producing a 650 nm pump beam. Both the output of the OPerA Solo as well as the remainder of the originally transmitted 800 nm light are directed into a commercial transient absorption spectrometer (Ultrafast Systems Helios, Sarasota, Florida). The pump beam is chopped at 500 Hz before being depolarized and focused with a 350 mm focal length lens to the sample position. The remaining 800 nm light is first passed onto a mechanical delay stage before being focused onto a translating CaF_2 crystal to generate a visible white light continuum from 425 to 850 nm. The white light is then filtered to remove any remaining fundamental light and split into the probe and reference beams. The reference beam is then reflected into a separate camera to account for jitter and intensity fluctuations. Ultrafast data (ΔOD (λ, t)) for each sample were collected by averaging 3 scans with 2 s of averaging at each time delay and corrected with a polynomial to account for the temporal chirp. Samples were held in 2 mm quarts cuvettes (FireflySci, Inc., Staten Island, New York).

Dynamic light scattering (DLS) and transmission electron microscopy (TEM) were used to characterize the morphological properties of the encapsulated fluorophores. Particle size and polydispersity index (PDI) were measured utilizing a Malvern Instrument Zetasizer Nano ZS using a 633 nm wavelength He–Ne laser with a detector angle of 173° at 25° C. For DLS, the samples were used without any treatment or dilution.

Synthesis:

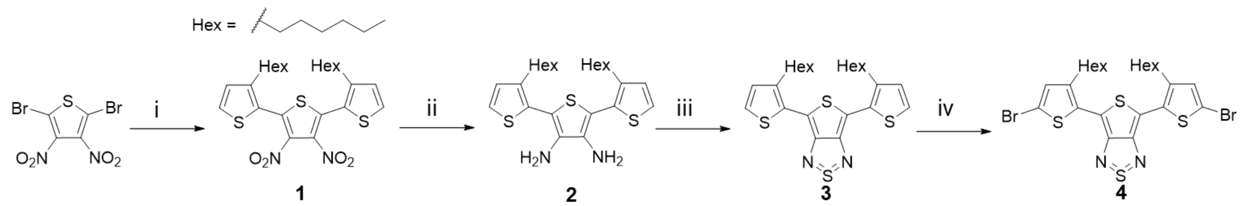

Scheme 1: i) 2-(3-hexylthiophen-2-yl)-4,4,5,5-tetramethyl-1,3,2-dioxaborolane, Pd^0 tetrakis, aq. K_2CO_3, Tol:EtOH, 100^{o} C for 24 hours; ii) $SnCl_2(H_2O)_2$, DCM:EtOH, conc. HCl, 25^{o} C for 3 days; iii) TMSCl, thionylaniline, Pyridine, 25^{o} C for 18 hours; iv) NBS, DMF, 0^{o} C to 25^{o} C for 18 hours

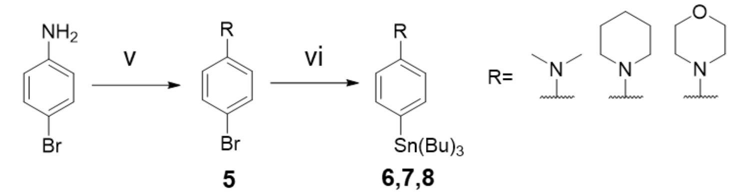

Scheme 2: v) 4-bromoaniline, SDS, $NaHCO_3$, 1,5-dibromopentane, H_2O, 80^{o} C for 18 hours; vi) n-BuLi, tri-n-butyltin chloride, THF, -78^{o} C to 25^{o} C for 4 hours

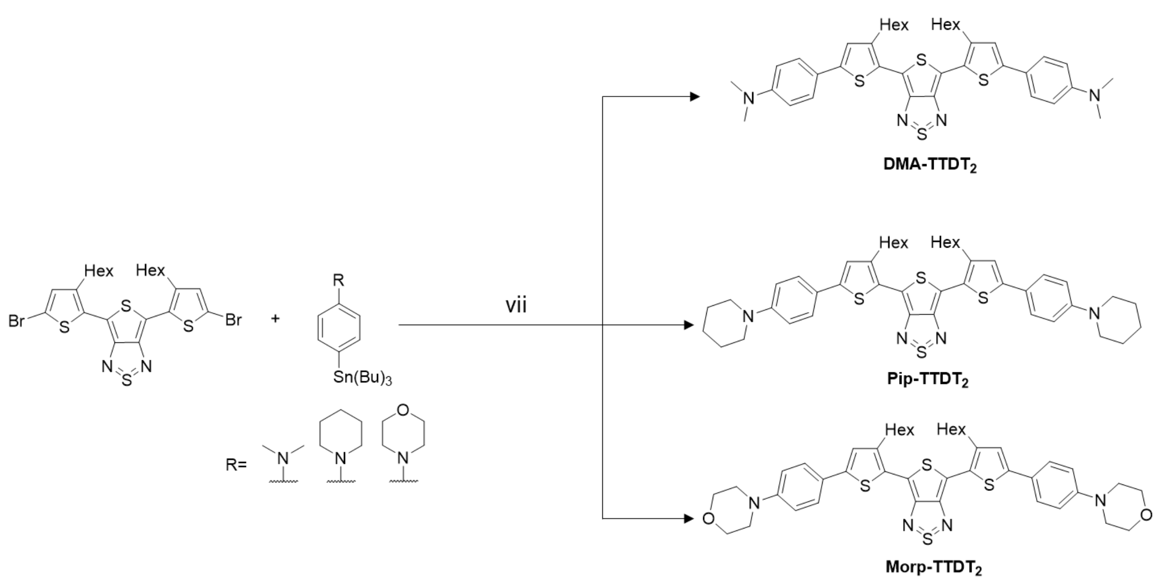

Scheme 3: vii) $PdCl_2(PPh_3)_2$, Toluene, 110^{o} C, 24 hours

Synthesis of **3,3''-dihexyl-3',4'-dinitro-2,2':5',2''-terthiophene** (**1**)[11]: 2,5-dibromo-3,4-dinitrothiophene (1.54 mmol/511 mg) and Pd^0 tetrakis (0.154 mmol/176 mg) were added to a two-neck 50 mL RBF. The RBF was evacuated and refilled with N_2 for three cycles. The solids were dissolved in a 1:1 mixture of Toluene:EtOH (10 mL each). 2-(3-hexylthiophen-2-yl)-4,4,5,5-tetramethyl-1,3,2-dioxaborolane (3.38 mmol/1.01 mL) was then added to the RBF. K_2CO_3 (6.16 mmol/851 mg) was dissolved in 2 mL of H_2O and was then added to the RBF. The reaction mixture was allowed to stir at 100^o C for 24 hours. The crude product was washed with H_2O and extracted with DCM and dried with $MgSO_4$. The product was purified via column chromatography using 4:1 Hexanes:DCM as the eluent to afford 575 mg (73% yield) of product as a yellow oil.

^{1}H NMR (400 MHz, $CDCl_3$) δ (ppm): 7.50 (d, J = 5.1 Hz, 2H), 7.04 (d, J = 5.3 Hz, 2H), 2.59 (t, J = 7.8 Hz 4H), 1.66-1.53 (m, 4H), 1.33-1.21 (m, 12 H), 0.87 (t, J = 6.4 Hz 6H).

Synthesis of **3,3''-dihexyl-[2,2':5',2''-terthiophene]-3',4'-diamine** (**2**)[11]: 3,3''-dihexyl-3',4'-dinitro-2,2':5',2''-terthiophene (1.13 mmol/575 mg) was added to a 100 mL RBF. The RBF was evacuated and refilled with N_2 for three cycles after which 7 mL of DCM (0.16 M) and 7 mL of EtOH (0.16 M) was added. $SnCl_2(H_2O)_2$ (11.3 mmol/2.54 g) was added to a separate RBF which was also evacuated and refilled with N_2 for three cycles and was then dissolved with 11.3 mL of EtOH (1 M) and 8.4 mL of conc. HCl (1.35 M). The $SnCl_2(H_2O)_2$ solution was then added to the RBF containing the 3,3''-dihexyl-3',4'-dinitro-2,2':5',2''-terthiophene and was allowed to stir at 25^o C for three days. The product was obtained by washing with 1 M NaOH and extracted with DCM before being dried with $MgSO_4$. The product was obtained in quantitative yields and was used without further purification.

Synthesis of **TTD-HexT$_2$** (**3**)[11]: 3,3''-dihexyl-[2,2':5',2''-terthiophene]-3',4'-diamine (1.47 mmol/700 mg) was added to a 100 mL RBF. The RBF was evacuated and refilled with N_2 for three cycles. The diamine was then dissolved with 8 mL of pyridine (0.2 M) and allowed to stir. TMSCl (10.3 mmol/1.3 mL) was added dropwise to the RBF followed by thionylaniline (2.94 mmol/0.33 mL). The reaction mixture immediately turns dark blue and is allowed to stir at 25^o C for 18 hours. The crude product is washed with 1 M HCl and extracted with DCM before being dried with $MgSO_4$. The product was purified with column chromatograph using 1:1 Hexanes/DCM as the eluent to give 350 mg (49% yield) of product as a blue solid.

^{1}H NMR (400 MHz, $CDCl_3$) δ (ppm): 7.35 (d, J = 5.3 Hz, 2H), 7.02 (d, J = 5.2 Hz, 2H), 2.92 (t, J = 7.9 Hz 4H), 1.77-1.69 (m, 4H), 1.34-1.30 (m, 12H), 0.93-0.89 (m, 6H).

Synthesis of **TTD-HexT$_2$-Br$_2$** (**4**): TTD-HexT$_2$ (0.36 mmol/170 mg) was added to a 50 mL RBF and was evacuated and refilled with N_2 for three cycles. 12 mL of DMF (0.03 M) was added and the solution was allowed to cool to 0^o C. NBS (0.79 mmol/140 mg) was added to a separate RBF which was evacuated and refilled with N_2 also. The NBS was dissolved with 8 mL of DMF (0.1 M) and was then added to the RBF with TTD-HexT$_2$. The reaction mixture was allowed to warm up to 25^o C and stir for 18 hours. The crude product was washed with H_2O and extracted with DCM before being dried with $MgSO_4$. The product was purified with column chromatography using 9:1 Hexanes:DCM as the eluent to give 60 mg (27% yield) as a blue solid.

^{1}H NMR (400 MHz, $CDCl_3$) δ (ppm): 6.95 (s, 2H), 2.84 (t, J = 7.8 Hz 4H), 1.74-1.65 (m, 4H), 1.34-1.29 (m, 12H), 0.91-0.82 (m, 6H).

Synthesis of **1-(4-bromophenyl)piperidine** (**5**): 4-bromoaniline (5.8 mmol/1 g), sodium dodecyl sulfate (SDS, 58 mg), and $NaHCO_3$ (13.9 mmol/1.16 g) were added to a 100 mL RBF. The RBF was evacuated and refilled with N_2 for three cycles. 58 mL of H_2O (0.1 M) were added to the RBF which was allowed to heat at 80^o C for 5 minutes. After 5 minutes, 1,5-dibromopentane (6.9 mmol/0.94 mL) was added and the reaction mixture was allowed to stir at 80^o C for 18 hours. The reaction mixture was allowed to cool to room temperature and the crude product was extracted with EtOAc and dried with $MgSO_4$. The product was purified with column chromatography using 100% Hexanes as the eluent to afford 914 mg (66% yield) of product as a white crystalline solid.

^{1}H NMR (400 MHz, $CDCl_3$) δ (ppm): 7.31 (d, J = 9.1 Hz, 2H), 6.79 (d, J = 9.3 Hz, 2H), 3.13-3.10 (m, 4H), 1.72-1.66 (m, 4H), 1.59-1.55 (m, 2H).

Synthesis of **N,N-dimethyl-4-(tributylstannyl)aniline** (**6**): N,N-dimethyl-4-bromoaniline (0.49 mmol/100 mg) was added to a 50 mL RBF which was evacuated and refilled with N_2 for three cycles. 3 mL of THF (0.2 M) was added to the RBF and was allowed to cool to -78^o C. n-BuLi (0.59 mmol/0.24 mL) was then added dropwise and the reaction mixture was allowed to stir at -78^o C for 30 minutes. Tri-n-butyltin chloride (0.54 mmol/0.15 mL) was added and the reaction mixture was allowed to warm to 25^{o}C and stir for 4 hours. The product washed with cold H_2O and extracted with Et_2O and dried with $MgSO_4$. The product was obtained as a viscous oil confirmed by TLC (100% Hexanes) and was used without further purification.

Synthesis of **1-(4-(tributylstannyl)phenyl)piperidine** (**7**): 1-(4-bromophenyl)piperidine (0.46 mmol/110 mg) was added to a 50 mL RBF which was evacuated and refilled with N_2 for three cycles. 3 mL of THF (0.2 M) was added to the RBF and was allowed to cool to -78^o C. n-BuLi (0.55 mmol/0.22 mL) was then added dropwise and the reaction mixture was allowed to stir at -78^o C for 30 minutes. Tri-n-butyltin chloride (0.51 mmol/0.14 mL) was added and the reaction mixture was allowed to warm to 25^{o}C and stir for 4 hours. The product washed with cold H_2O and extracted with Et_2O and dried with $MgSO_4$. The product was obtained as a viscous oil confirmed by TLC (100% Hexanes) and was used without further purification.

Synthesis of **4-(4-(tributylstannyl)phenyl)morpholine** (**8**): 4-(4-bromophenyl)morpholine (0.41 mmol/100 mg) was added to a 50 mL RBF which was evacuated and refilled with N_2 for three cycles. 2 mL of THF (0.2 M) was added to the RBF and was allowed to cool to -78^o C. n-BuLi (0.50 mmol/0.20 mL) was then added dropwise and the reaction mixture was allowed to stir at -78^o C for 30 minutes. Tri-n-butyltin chloride (0.45 mmol/0.12 mL) was added and the reaction mixture was allowed to warm to 25^{o}C and stir for 4 hours. The product washed with cold H_2O and extracted with Et_2O and dried with $MgSO_4$. The product was obtained as a viscous oil confirmed by TLC (100% Hexanes) and was used without further purification.

Synthesis of **DMA-TTDT$_2$**: TTD-HexT$_2$-Br$_2$ (0.1 mmol/60 mg) and $PdCl_2(PPh_3)_2$ (0.01 mmol/10 mg) were added to a two-neck 50 mL RBF with a condenser which was evacuated and refilled with N_2 for three cycles. 8 mL of Toluene (0.0125 M) was added followed by N,N-dimethyl-4-(tributylstannyl)aniline (0.22 mmol/90 mg) and the reaction mixture was heated to 110^o C and allowed to stir for 24 hours. Toluene was removed and the crude product was precipitated out with Hexanes and collected with vacuum filtration. The product was further purified with column chromatography using 100% DCM as the eluent to give 26 mg (37% yield) of product as a dark green solid.

^{1}H NMR (400 MHz, $CDCl_3$) δ (ppm): 7.57 (d, J = 8.2 Hz, 4H), 7.08 (s, 2H), 6.74 (d, J = 8.3 Hz, 4H), 3.01 (s, 12H), 2.94-2.91 (m, 4H), 1.83-1.75 (m, 4H), 1.52-1.47 (m, 4H), 1.38-1.34 (m, 8 H), 0.92-0.89 (brt, 6H).

^{13}C NMR (101 MHz, $CDCl_3$) δ (ppm): 156.59, 150.25, 145.01, 140.80, 127.15, 126.72, 124.22, 122.50, 112.57, 112.43, 40.59, 31.96, 30.92, 30.03, 29.69, 22.84, 14.29.

HRMS (ESI) calcd. For [M+H]+ m/z: $C_{40}H_{48}N_4S_4$: 712.2762; Found: 712.2760

Synthesis of **Pip-TTDT$_2$**: TTD-HexT$_2$-Br$_2$ (0.1 mmol/60 mg) and $PdCl_2(PPh_3)_2$ (0.01 mmol/10 mg) were added to a two-neck 50 mL RBF with a condenser which was evacuated and refilled with N_2 for three cycles. 10 mL of Toluene (0.01 M) was added followed by 1-(4-(tributylstannyl)phenyl)piperidine (0.22 mmol/99 mg) and the reaction mixture was heated to 110^o C and allowed to stir for 24 hours. Toluene was removed and the crude product was precipitated out with Hexanes and collected with vacuum filtration. The product was further purified with column chromatography using 100% DCM as the eluent to give 30 mg (38% yield) of product as a dark green solid.

^{1}H NMR (400 MHz, $CDCl_3$) δ (ppm): 7.55 (d, J = 8.9 Hz, 4H), 7.10 (s, 2H), 6.94 (d, J = 8.9 Hz, 4H), 3.23 (t, J = 6.1 Hz, 8H), 2.93 (t, J = 8.0 Hz, 4H), 1.82-1.76 (m, 4H), 1.75-1.69 (m 8H), 1.63-1.59 (m, 4H), 1.54-1.47 (m, 4H), 1.38-1.34 (m, 8H), 0.91 (t, J = 7.0 Hz, 6H).

^{13}C NMR (101 MHz, $CDCl_3$) δ (ppm): 156.49, 151.56, 144.53, 140.69, 127.40, 126.44, 124.58, 124.50, 116.03, 112.36, 50.05, 31.81, 30.76, 29.88, 29.54, 25.70, 24.32, 22.69, 14.14.

HRMS (ESI) calcd. For [M+H]+ m/z: $C_{46}H_{56}N_4S_4$: 792.3388; Found: 793.3450

Synthesis of **Morp-TTDT$_2$**: TTD-HexT$_2$-Br$_2$ (0.08 mmol/50 mg) and $PdCl_2(PPh_3)_2$ (0.008 mmol/5.6 mg) were added to a two-neck 50 mL RBF with a condenser which was evacuated and refilled with N_2 for three cycles. 8 mL of Toluene (0.01 M) was added followed by 4-(4-(tributylstannyl)phenyl)morpholine (0.17 mmol/80 mg) and the reaction mixture was heated to 110^o C and allowed to stir for 24 hours. Toluene was removed and the crude product was precipitated out with Hexanes and collected with vacuum filtration. The product was further purified with column chromatography using 100% DCM as the eluent to give 19.7 mg (31% yield) of product as a dark green solid.

^{1}H NMR (400 MHz, $CDCl_3$) δ (ppm): 7.58 (d, J = 8.8 Hz, 4H), 7.13 (s, 2H), 6.93 (d, J = 8.8 Hz, 4H), 3.88 (t, J = 4.8 Hz, 8H), 3.22 (t, J = 4.9 Hz, 8H), 2.93 (t, J = 7.6 Hz, 4H), 1.83-1.75 (m, 4H), 1.53-1.46 (m, 4H), 1.41-1.30 (m, 8H), 0.91 (t, J = 6.9 Hz 6H).

^{13}C NMR (101 MHz, $CDCl_3$) δ (ppm): 156.67, 150.90, 144.29, 140.89, 127.86, 126.68, 125.76, 125.05, 115.66, 112.56, 66.97, 49.02, 31.95, 30.90, 30.02, 29.68, 22.83, 14.28.

HRMS (ESI) calcd. For [M+H]+ m/z: $C_{44}H_{52}N_4O_2S_4$: 796.2973; Found: 797.3049

Synthesis of **PhPCL-PEG** polymer: Monomethoxy PEG-4000 (dehydrated by refluxing in toluene and further dried under vacuum) (1.00 g, 0.25 mmol), ε-caprolactone (1.275 g, 0.25 mmol), phenyl caprolactone (0.225 g, 0.25 mmol), 2-ethylhexanoate ($Sn(Oct)_2$) (190 mg, 0.25 mmol) were added in a clean RBF maintained in the glove box under inert atmosphere. The overall hydrophilic and hydrophobic percentage was maintained at 40% and 60 %, respectively. Anhydrous chlorobenzene (7.65 ml) and chloroform (1.5 ml) were added to the above mixture which was heated to 120 °C, and further stirred for 10 h. The reaction mixture was cooled down to room temperature, added dropwise into 10 ml of hexanes while stirring. A brownish yellow precipitate formed instantly. The mixture kept stirring for 30 more minutes, and stirring was stopped. The precipitate was allowed to settle, and hexanes was decanted from the mixture. The resulting brownish precipitate was redissolved in chloroform (5 ml) and added dropwise into 10 ml of hexanes, as mentioned in the previous step. To obtain a pure product the precipitation procedure was repeated three times. The resulting brownish yellow precipitate was dried under a high vacuum at 25 °C for 24 hours to obtain the pure product with a 70% yield (1 g).

^{1}H NMR (400 MHz, $CDCl_3$) δ 7.29, 7.20, 7.11, 4.05, 3.99, 3.64, 2.48, 2.30, 2.23, 2.11, 1.98, 1.64, 1.38.

GPC polymer characterization: M_n = 12,718 Da, M_w = 14,763 Da, M_z = 17,044 Da, M_p = 13,346 Da, M_w/M_n = 1.16

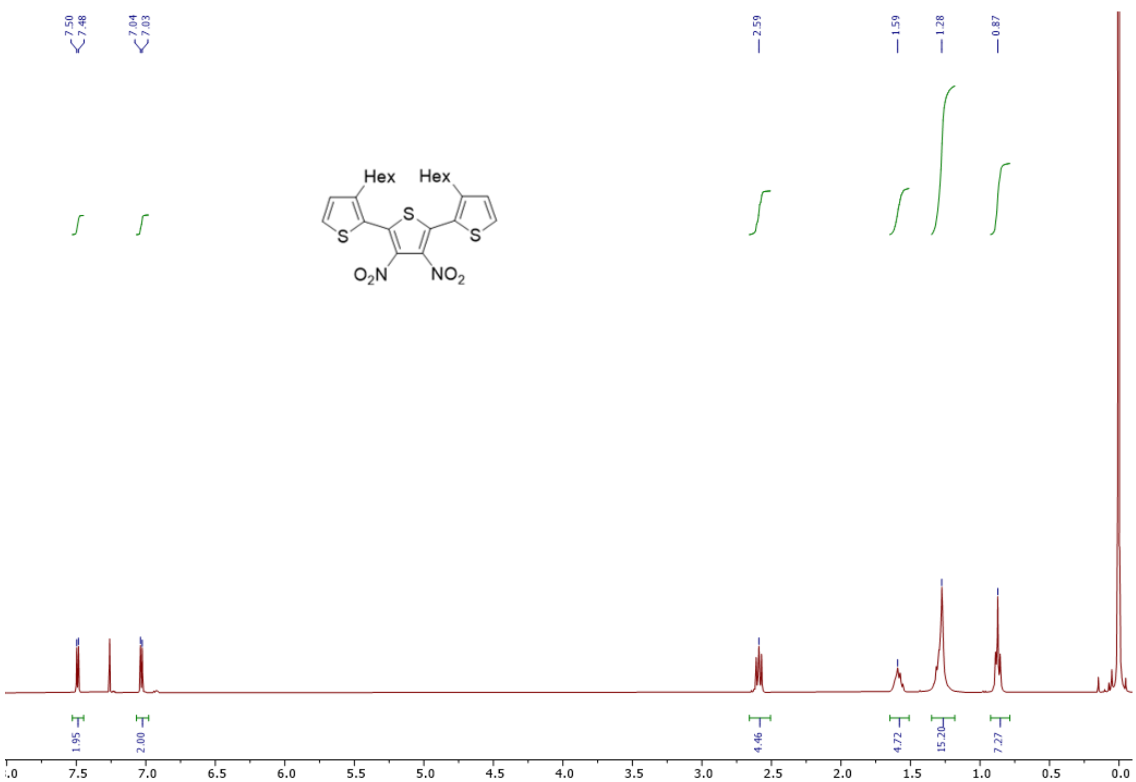

Figure S1: ^{1}H NMR of 3,3''-dihexyl-3',4'-dinitro-2,2':5',2''-terthiophene (**1**)

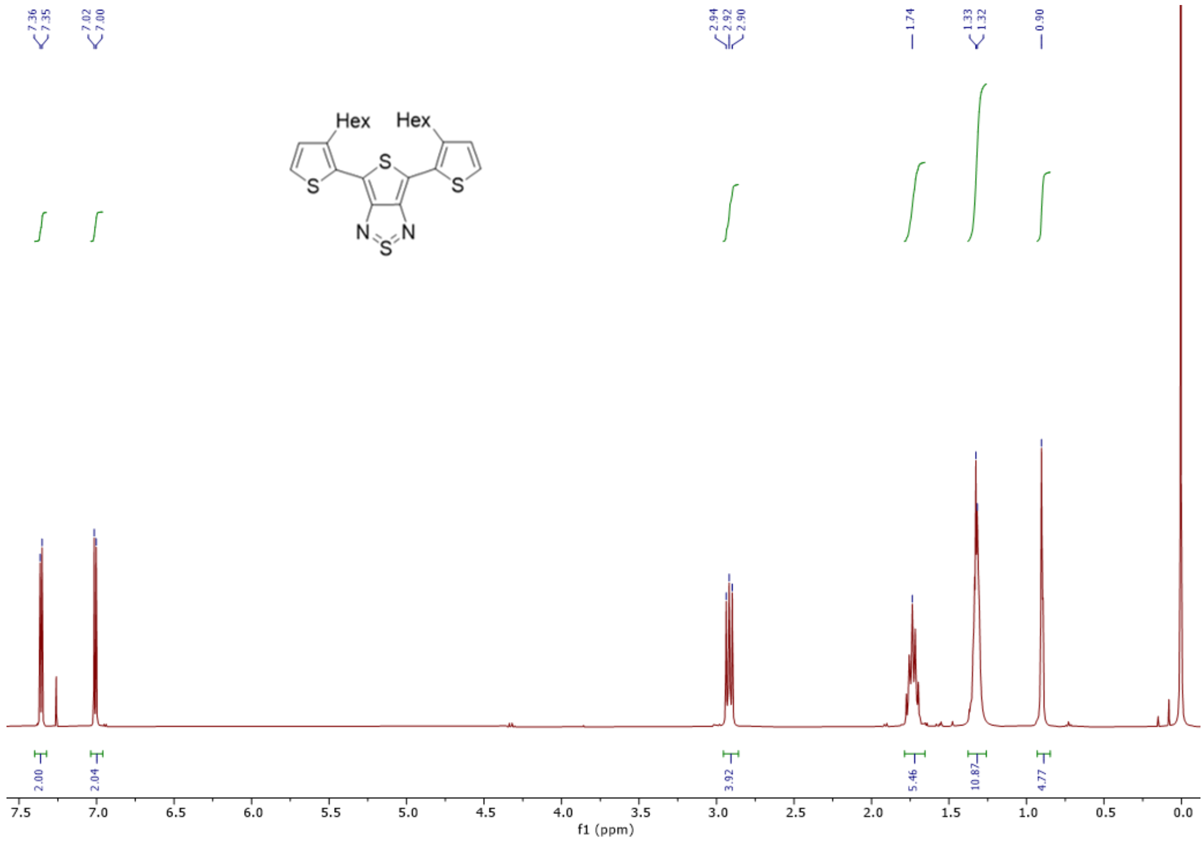

Figure S2: ^{1}H NMR of TTD-HexT_2 (**3**)

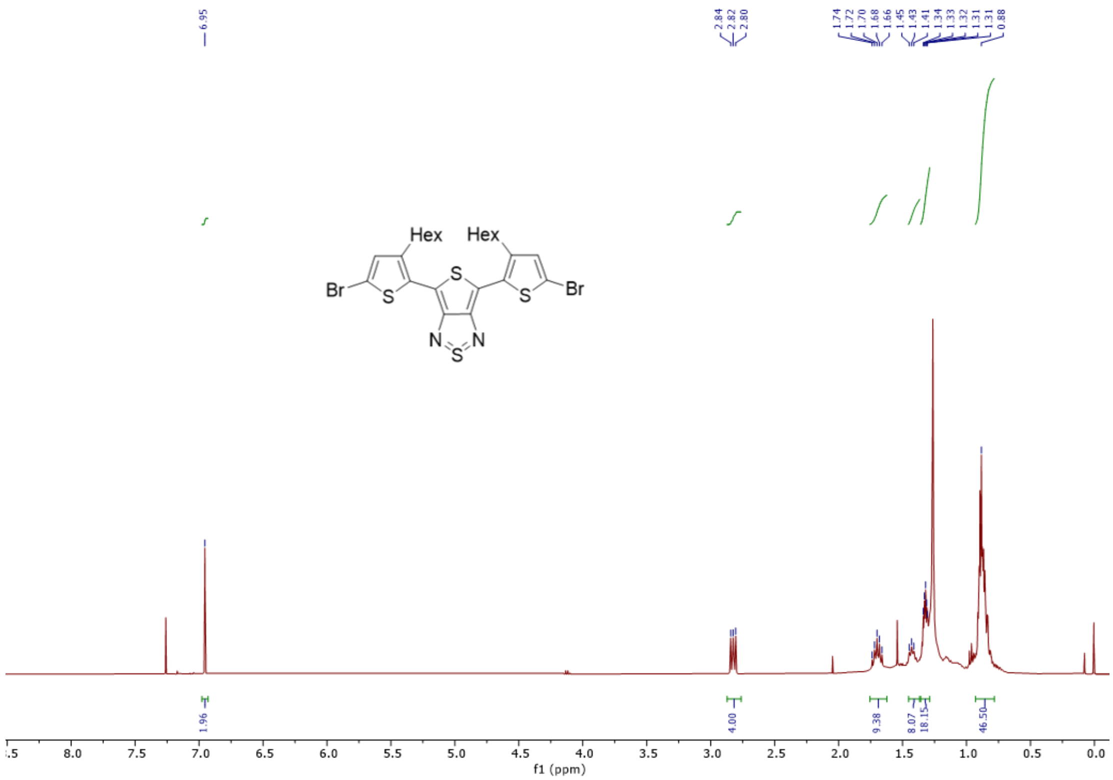

Figure S3: ^{1}H NMR of TTD-HexT$_2$-Br$_2$ (**4**); impurities: vacuum grease, ethyl acetate

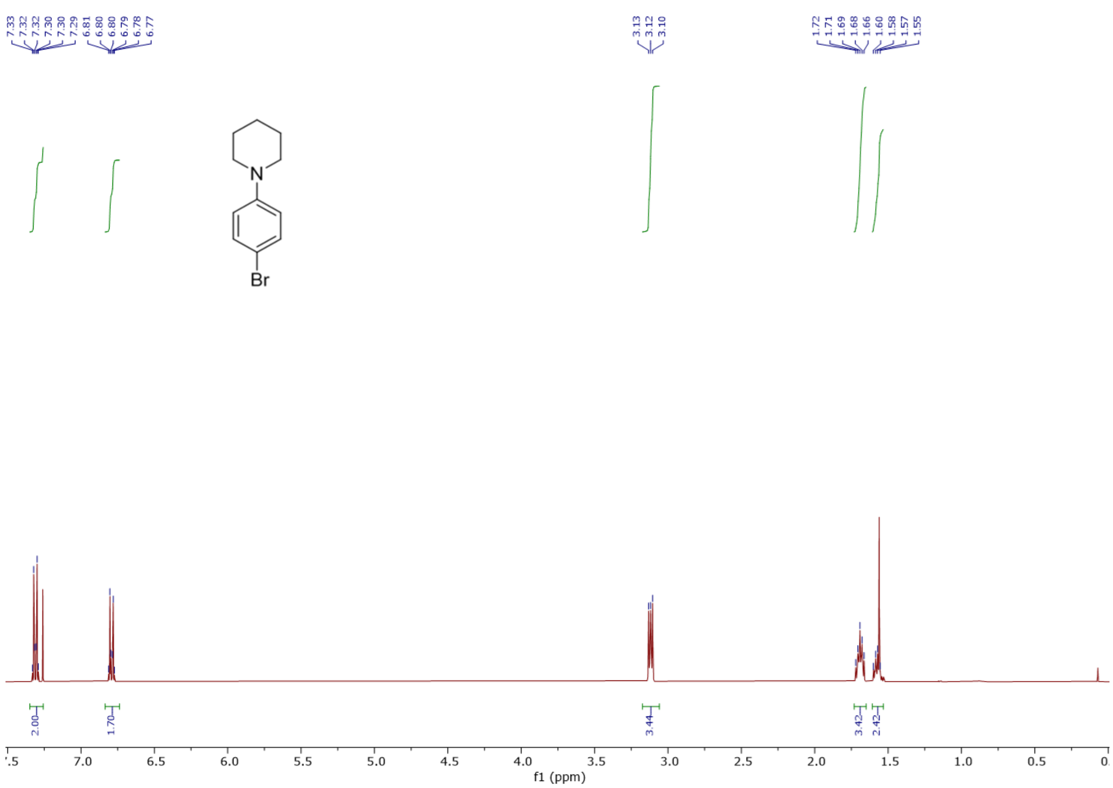

Figure S4: ^{1}H NMR of 1-(4-bromophenyl)piperidine (**5**)

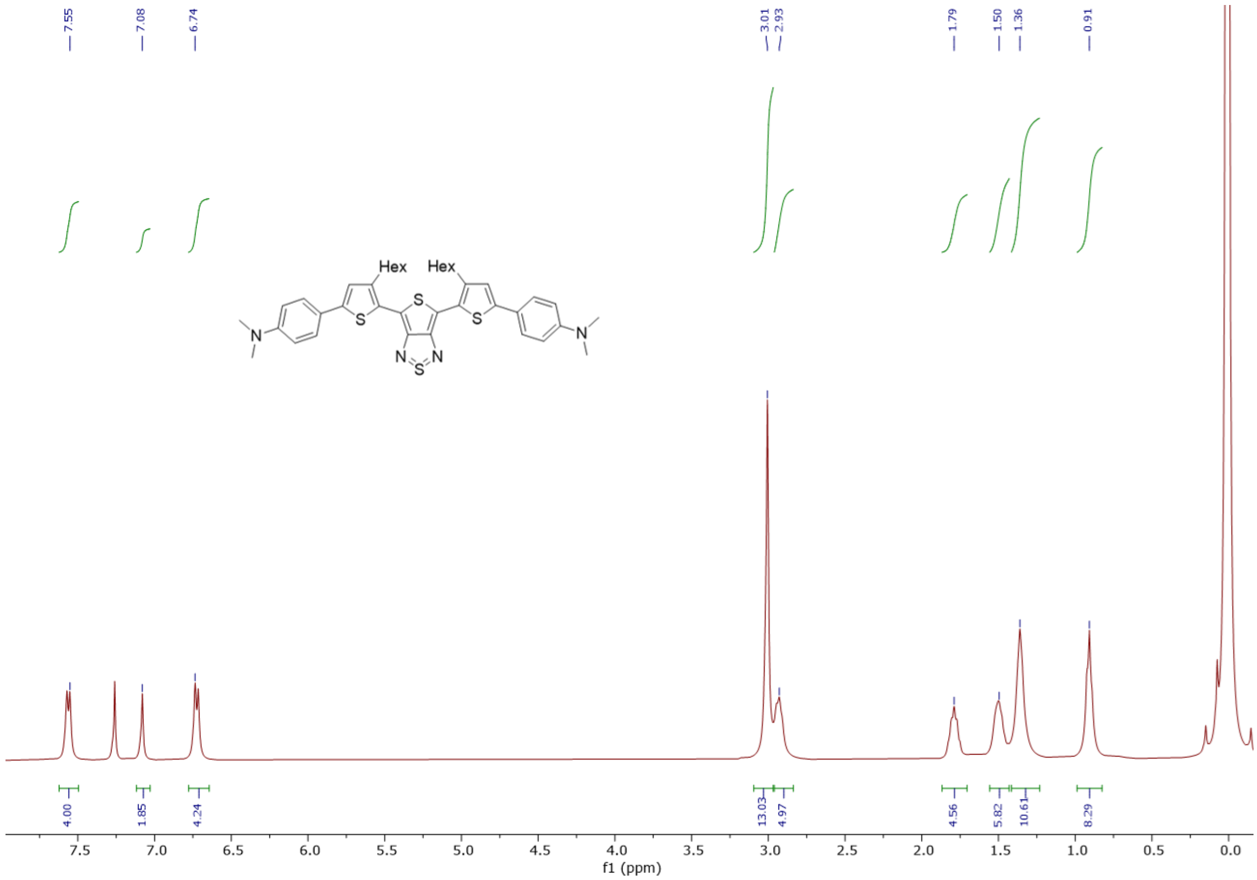

Figure S5: ^{1}H NMR of **DMA-TTDT$_2$**; impurities: silicon oil

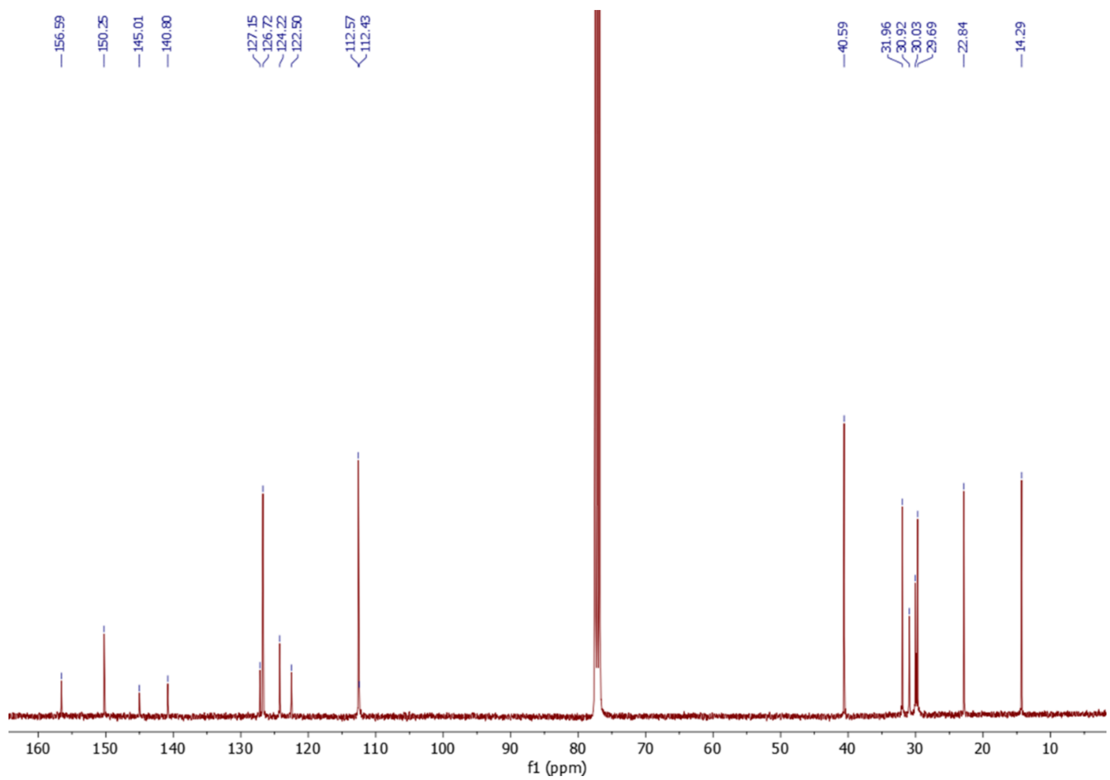

Figure S6: [13]C NMR of **DMA-TTDT$_2$**; impurities: silicon oil

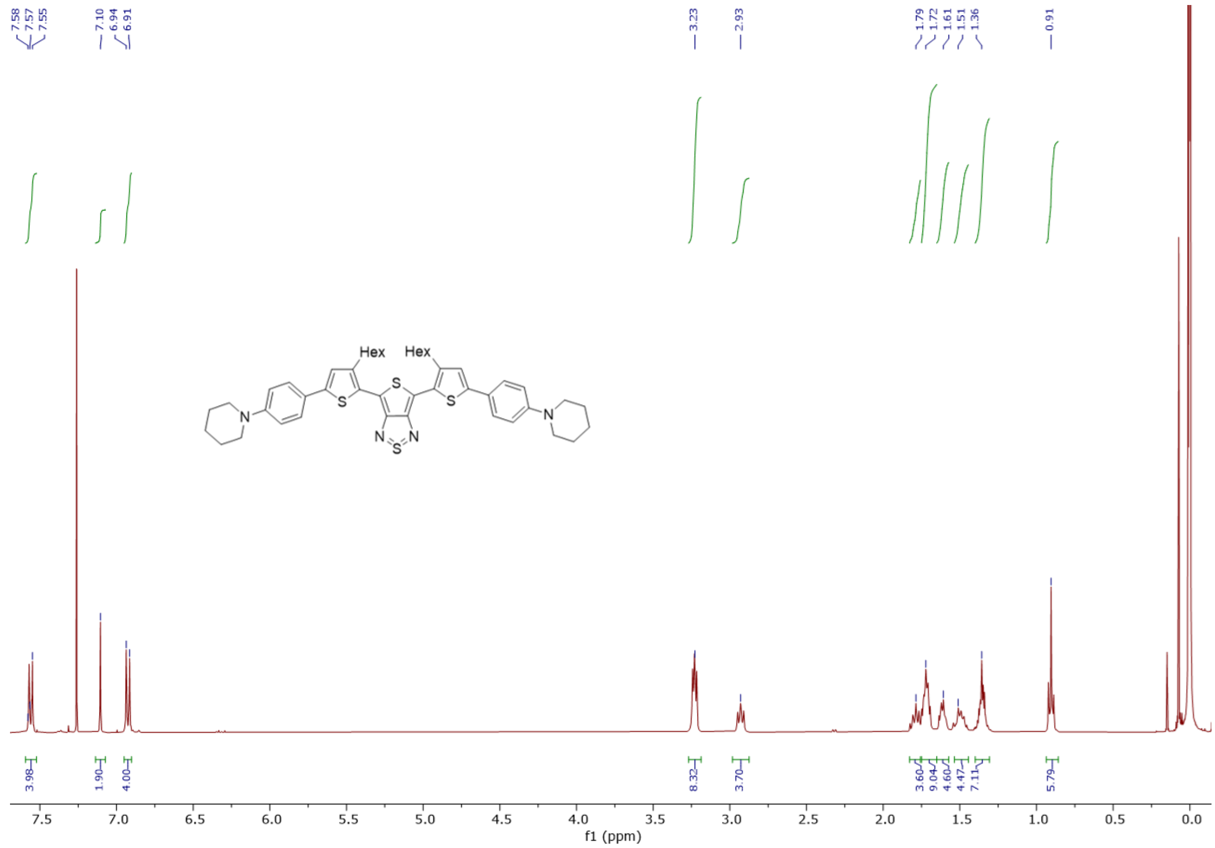

Figure S7: ^{1}H NMR of **Pip-TTDT$_2$**; impurities: silicon oil

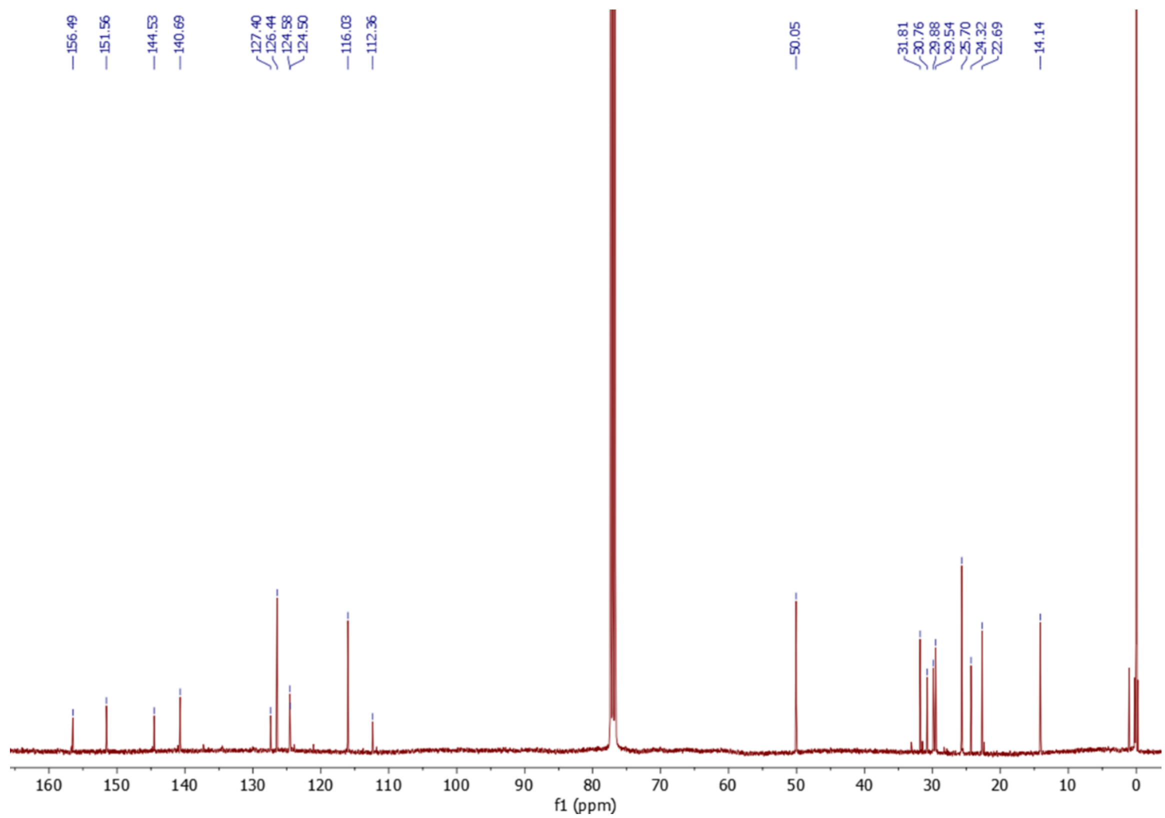

Figure S8: [13]C NMR of **Pip-TTDT$_2$**; impurities: silicon oil

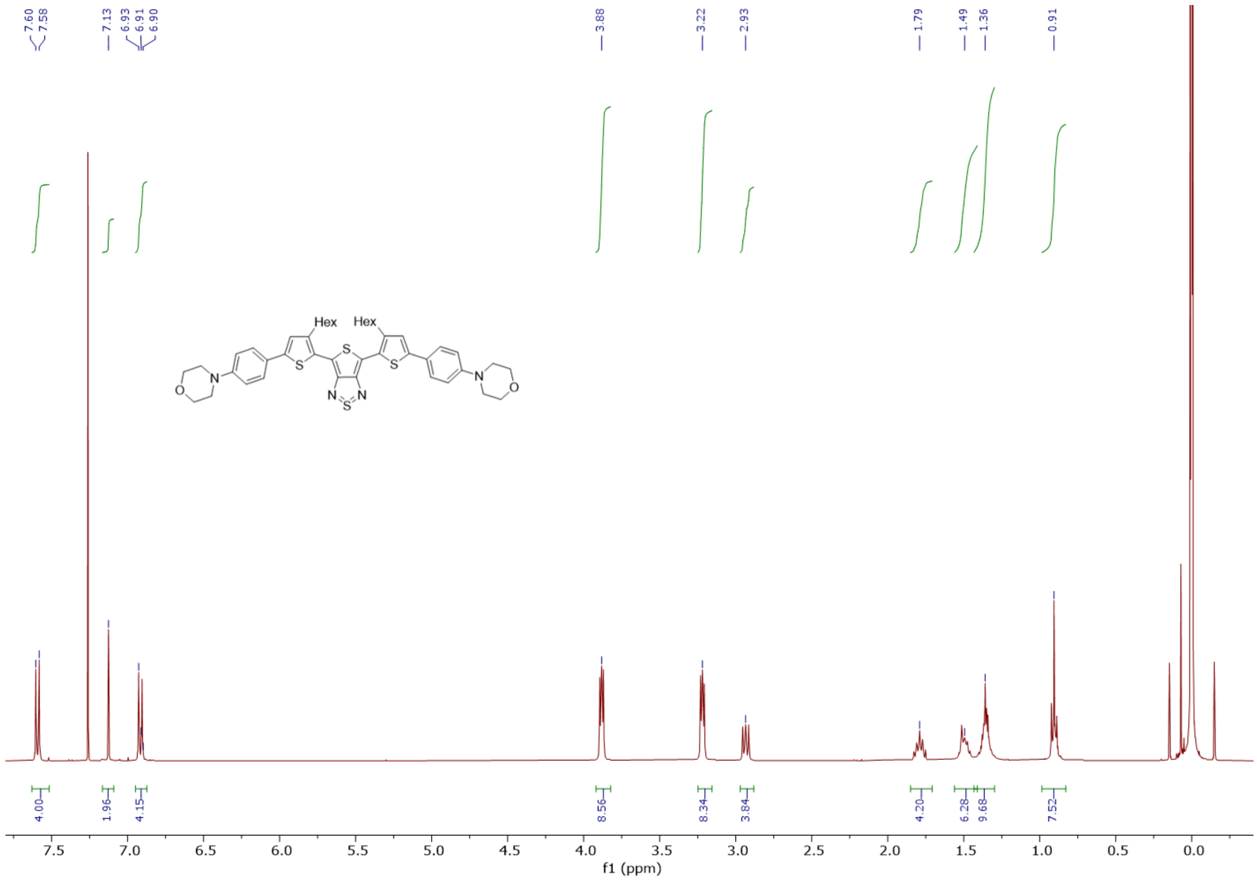

Figure S9: ^{1}H NMR of **Morp-TTDT₂**; impurities: silicon oil

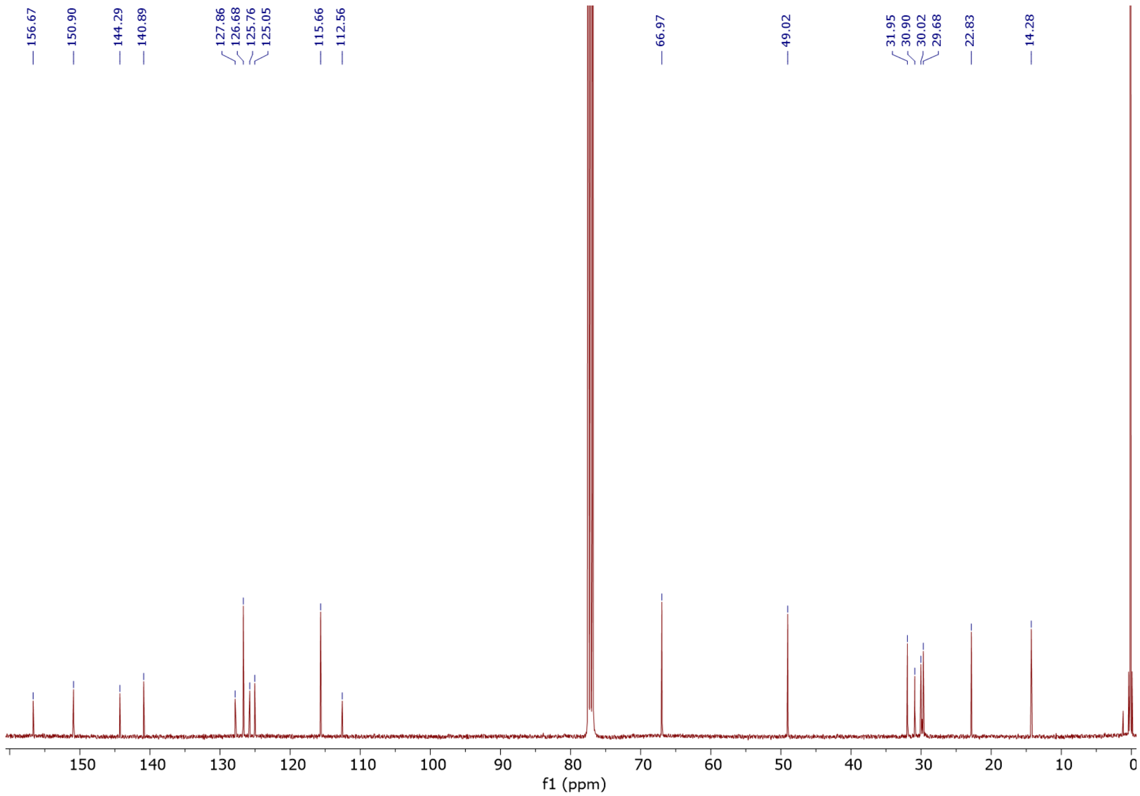

Figure S10: ^{13}C NMR of **Morp-TTDT$_2$**; impurities: silicon oil

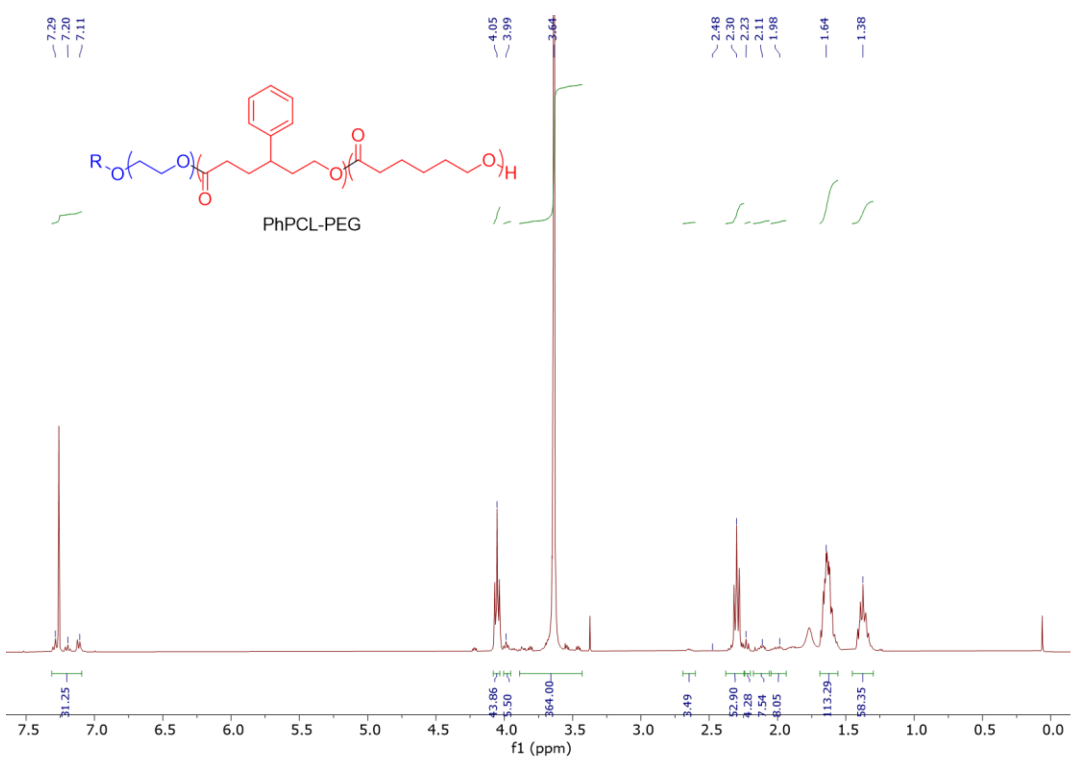

Figure S11: ^{1}H NMR and structure PhPCL-PEG polymer; GPC polymer characterization: M_n = 12,718 Da, M_w = 14,763 Da, M_z = 17,044 Da, M_p = 13,346 Da, M_w/M_n = 1.16

Photophysical Characterization:

Table S1: Absorbance values (in nm) of the $TTDT_2$ derivatives from both pH studies. Acetone/H_2O study was performed at a ratio of 6 mL acetone to 1 mL H_2O at the appropriate pH. Nanoparticle study was performed with 1 mL of a 1 mg/mL nanoparticle solution and 1 mL of H_2O at the appropriate pH.

	Acetone/H_2O			Nanoparticle		
	pH 7	**pH 5**	**pH 3**	**pH 7**	**pH 5**	**pH 3**
DMA-TTDT$_2$	725	729	729	720	729	740
Pip-TTDT$_2$	716	714	698	734	721	728
Morp-TTDT$_2$	704	703	703	721	714	713

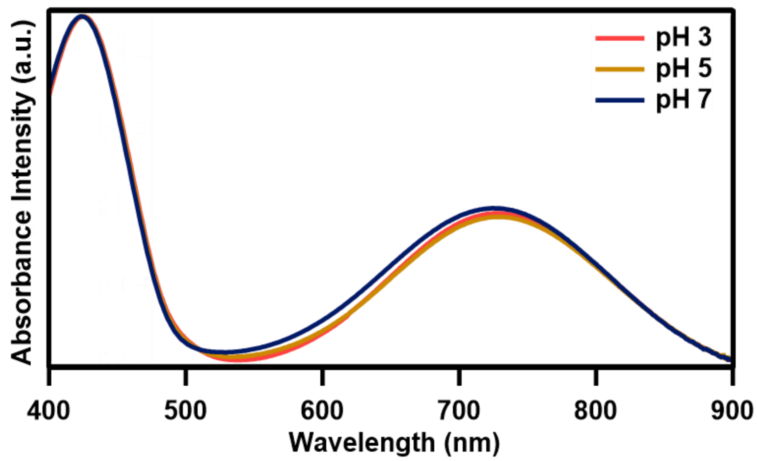

Figure S12: UV-Vis-NIR absorbance of **DMA-TTDT$_2$** in Acetone/H_2O in different pHs

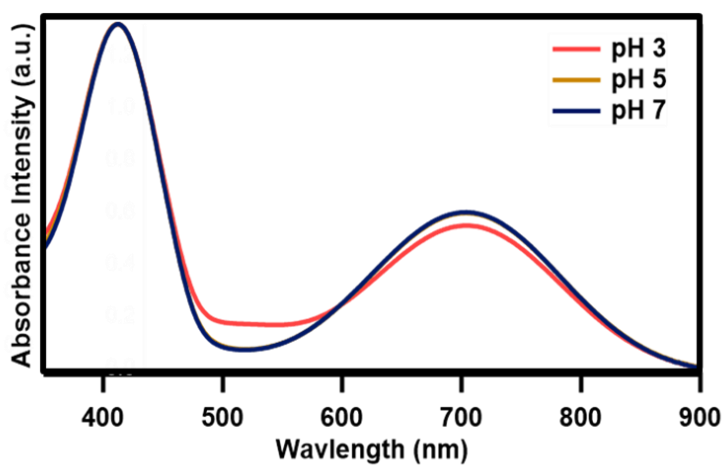

Figure S13: UV-Vis-NIR absorbance of **Morp-TTDT$_2$** in Acetone/H_2O in different pHs

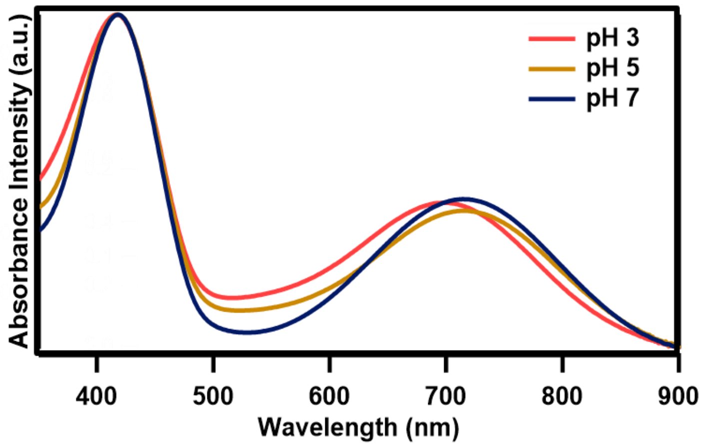

Figure S14: UV-Vis-NIR absorbance of **Pip-TTDT$_2$** in Acetone/H_2O in different pHs

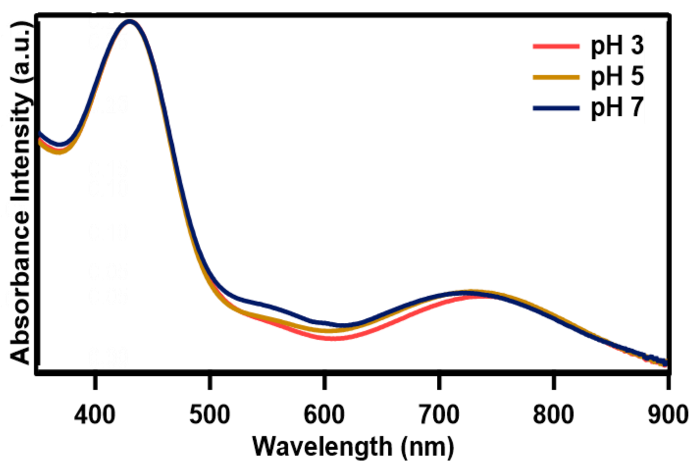

Figure S15: UV-Vis-NIR absorbance of **DMA-TTDT$_2$** nanoparticles in H_2O at different pHs

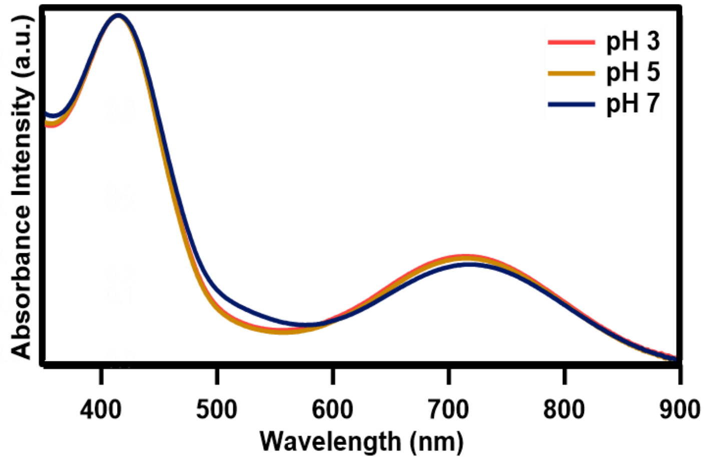

Figure S16: UV-Vis-NIR absorbance of **Morp-TTDT₂** nanoparticles in H_2O at different pHs

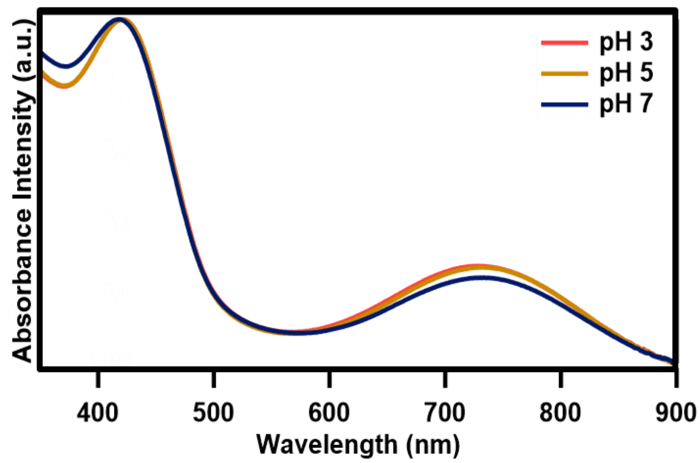

Figure S17: UV-Vis-NIR absorbance of **Pip-TTDT₂** nanoparticles in H_2O at different pHs

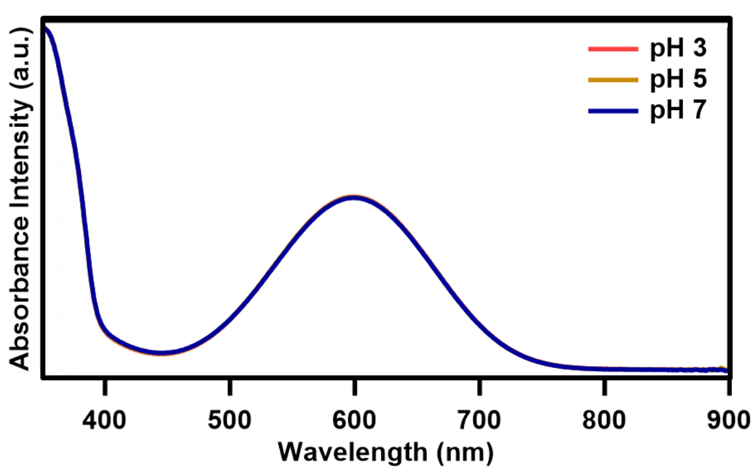

Figure S18: UV-Vis-NIR absorbance spectra of TTD-HexT_2 in Acetone/H_2O in different pHs

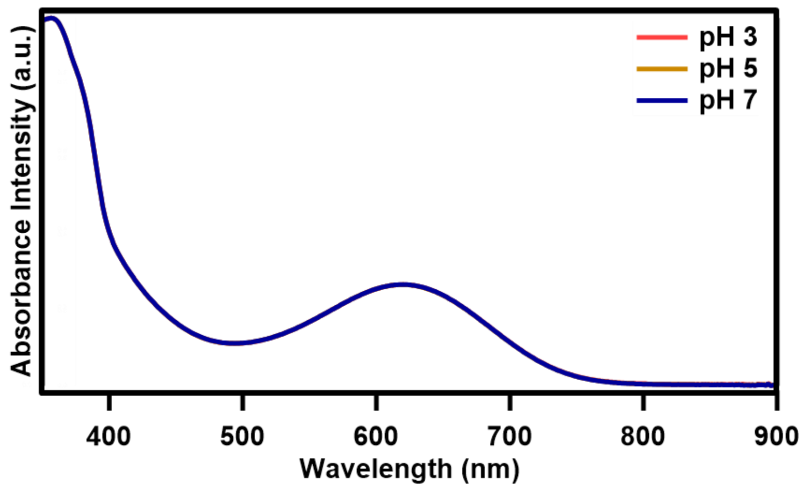

Figure S19: UV-Vis-NIR absorbance of TTD-HexT_2 nanoparticles in H_2O at different pHs

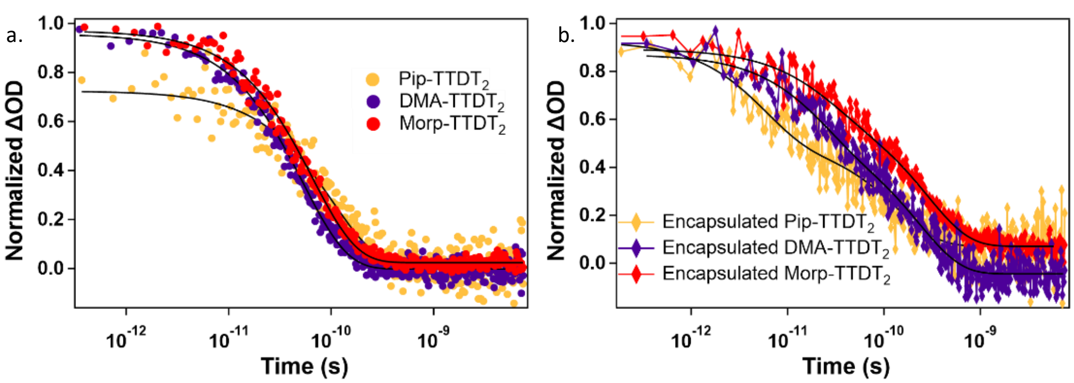

Figure S20: Excited state lifetime curves of the $TTDT_2$ derivatives in $CHCl_3$ (a) and encapsulated (b)

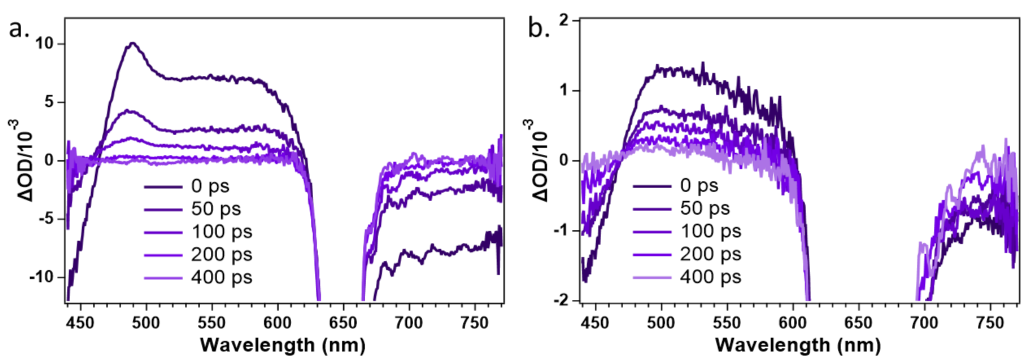

Figure S21: TAS spectra of **DMA-TTDT$_2$** in $CHCl_3$ (a) and encapsulated (b)

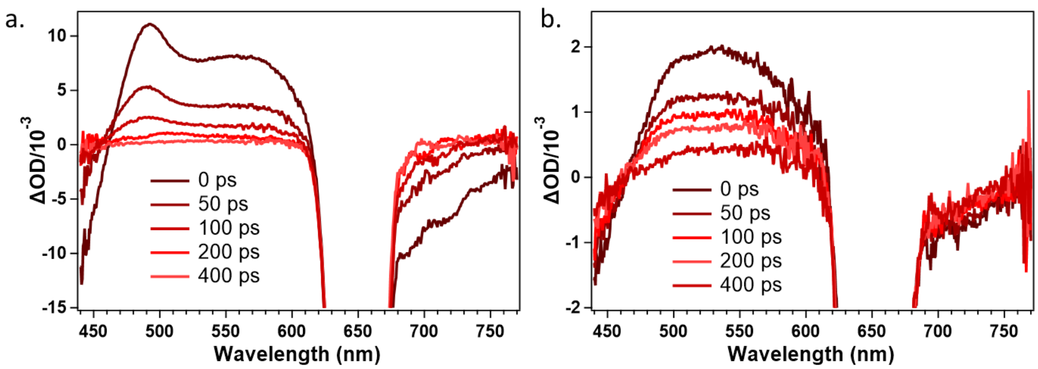

Figure S22: TAS spectra of **Morp-TTDT$_2$** in $CHCl_3$ (a) and encapsulated (b)

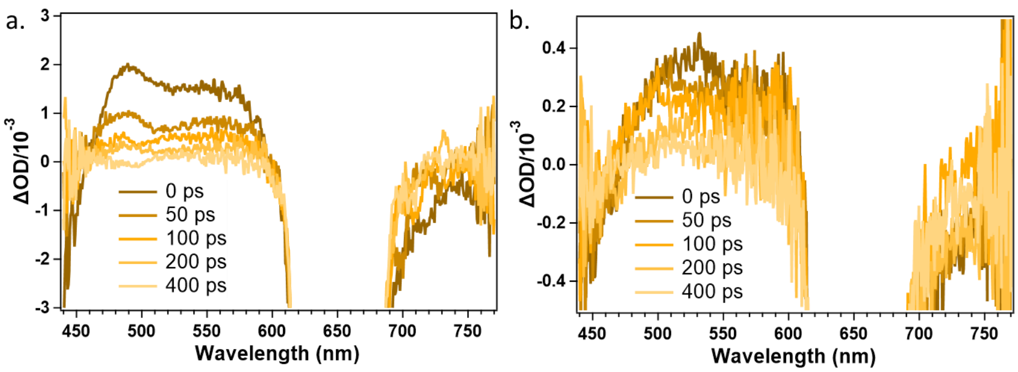

Figure S23: TAS spectra of **Pip-TTDT$_2$** in $CHCl_3$ (a) and encapsulated (b)

Nanoparticle Morphology:

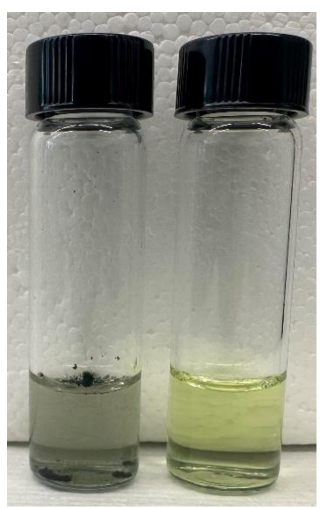

Figure S24: Image of **DMA-TTDT$_2$** in water (left vial) and encapsulated in PhPCL-PEG polymer (right vial)

Table S2: Nanoparticle size data for the $TTDT_2$ derivatives and the empty PhPCL-PEG polymer. For DLS, the measured standard deviations (±) are determined from the experiments being run in triplicate. For TEM, the standard deviations are calculated from the average measured size of each nanoparticle.

	DLS			TEM
	Intensity (nm)	**PDI**	**Number (nm)**	**(nm)**
DMA-$TTDT_2$	51.8 ± 1.22	0.122	21.7 ± 10.4	48.1 ± 14.0
Pip-$TTDT_2$	83.9 ± 6.29	0.218	23.0 ± 8.45	84.4 ± 22.7
Morp-$TTDT_2$	61.9 ± 2.74	0.172	21.7 ± 10.4	73.5 ± 21.8
Empty Polymer	124.5 ± 16.8	0.320	26.8 ± 5.93	90.8 ± 23.2

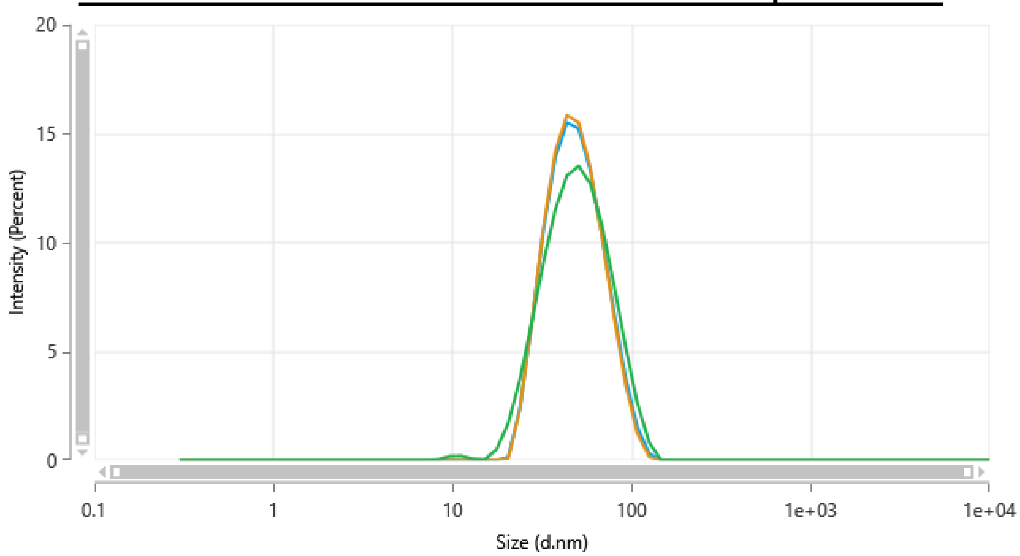

Figure S25: DLS spectra (intensity) of **DMA-$TTDT_2$** nanoparticles

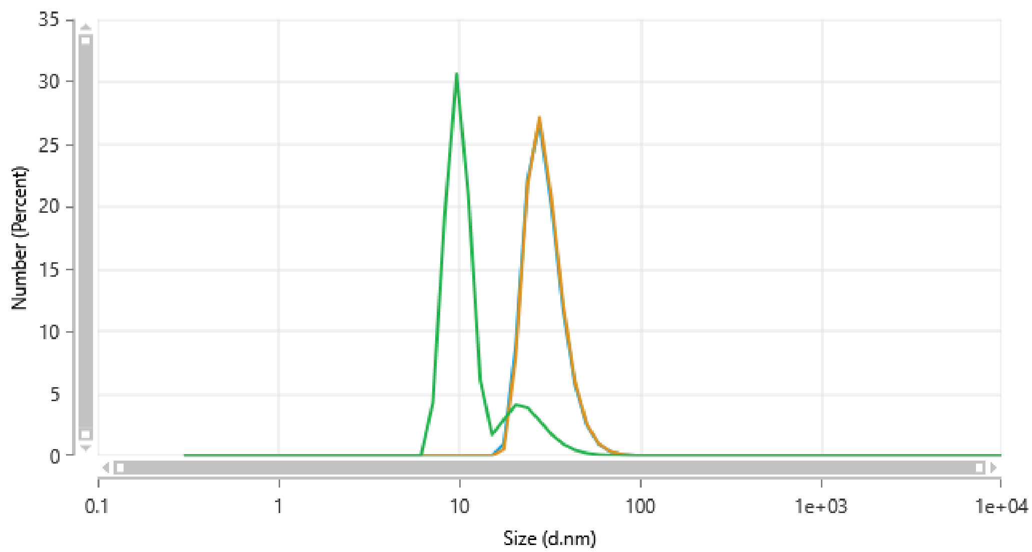

Figure S26: DLS spectra (number) of **DMA-TTDT$_2$** nanoparticles

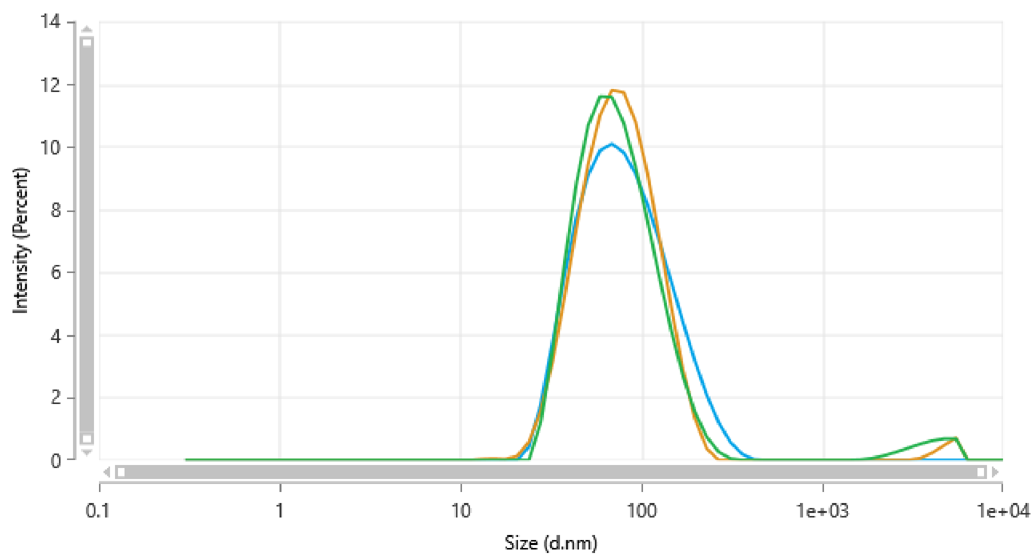

Figure S27: DLS spectra (intensity) of **Pip-TTDT$_2$** nanoparticles

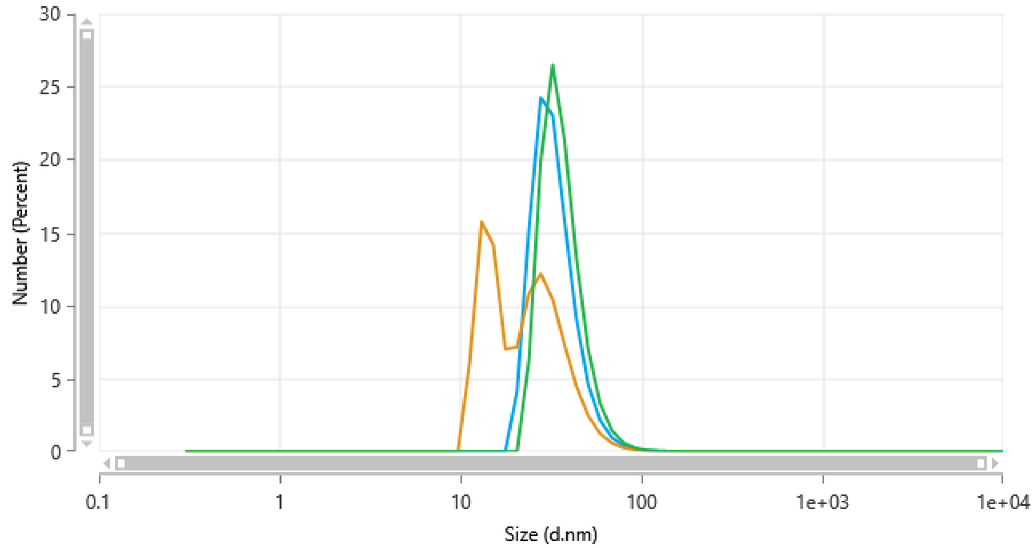

Figure S28: DLS spectra (number) of **Pip-TTDT$_2$** nanoparticles

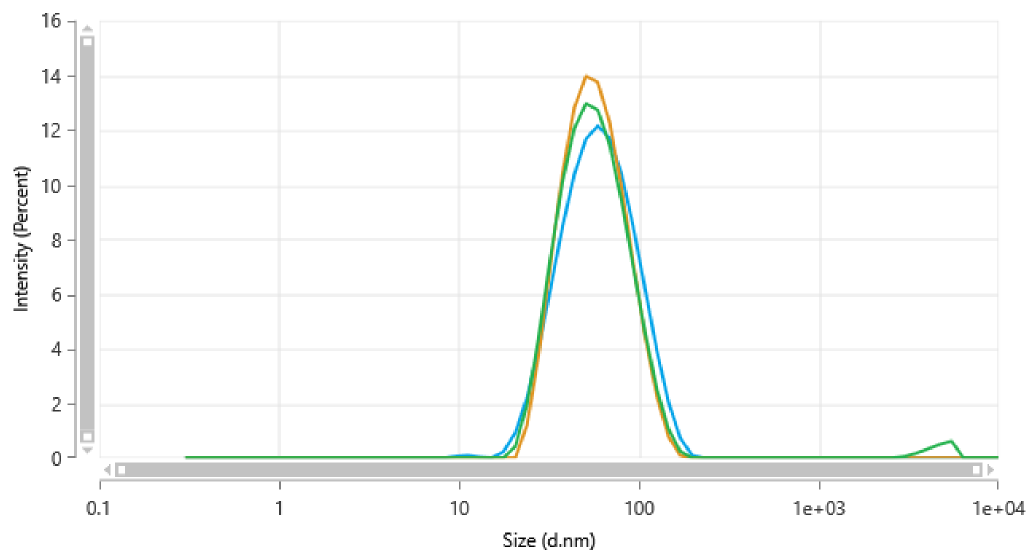

Figure S29: DLS spectra (intensity) of **Morp-TTDT$_2$** nanoparticles

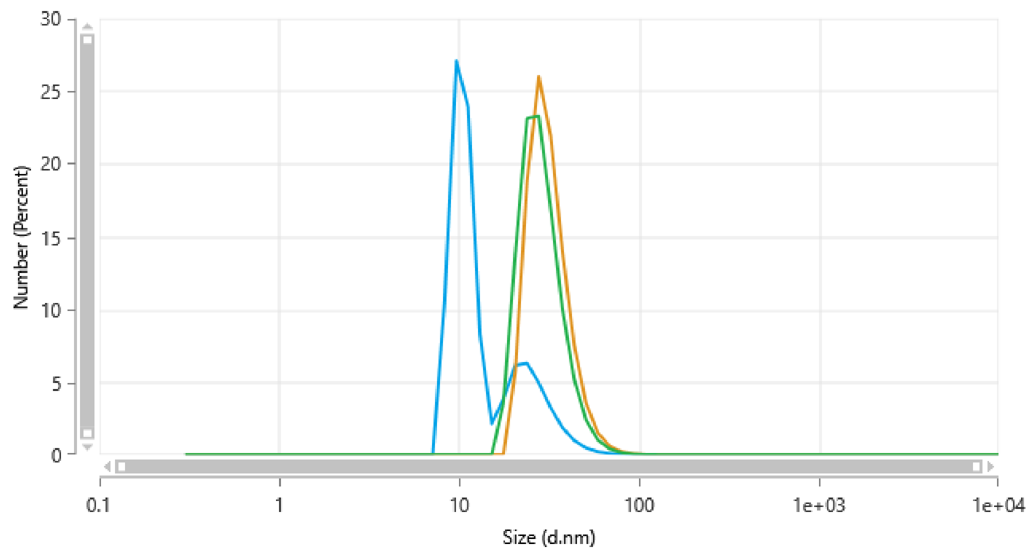

Figure S30: DLS spectra (number) of **Morp-TTDT$_2$** nanoparticles

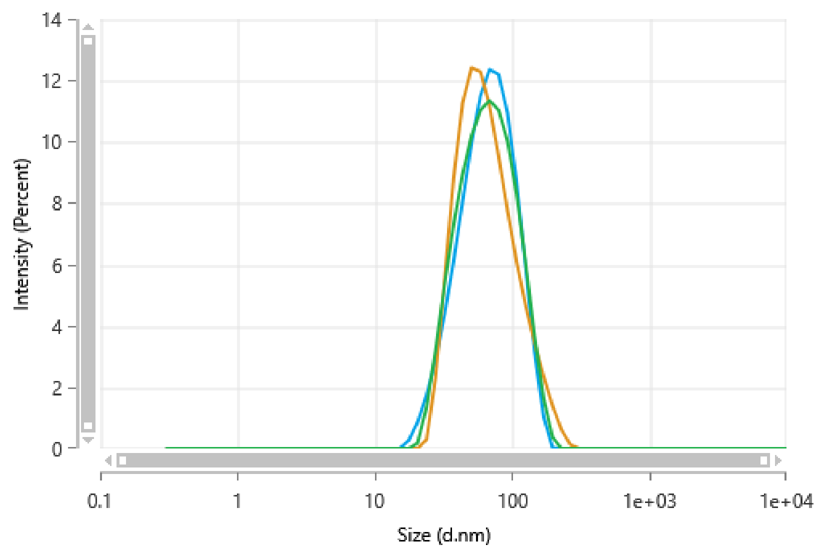

Figure S31: DLS spectra (intensity) of empty PhPCL-PEG nanoparticles

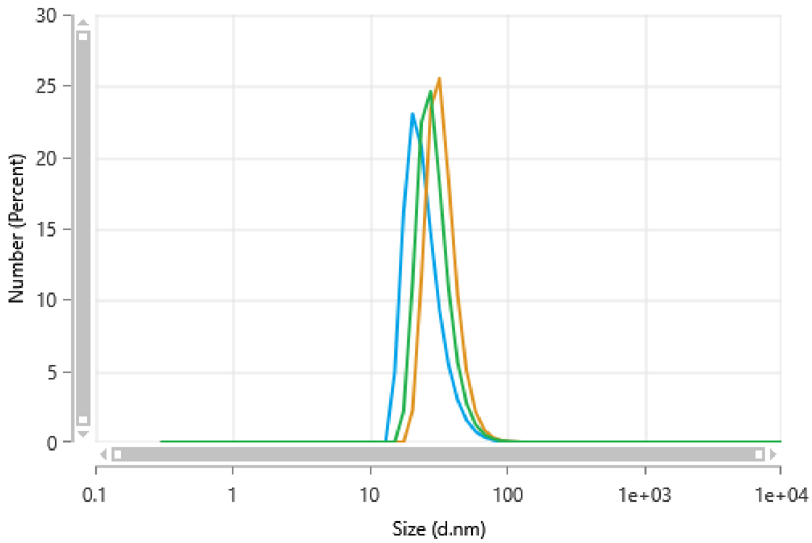

Figure S32: DLS spectra (number) of empty PhPCL-PEG nanoparticles

Photothermal Efficiency:

Photothermal properties of **Morp-TTDT$_2$** nanoparticles:

Initially, the photothermal properties of these nanoparticles were determined using high laser power (1.6 W), where we observed instability after the laser exposure (Fig. 33b). Because of this, the photothermal properties were measured at low laser power (0.4 W). The sample did not exhibit a significant change in UV-Vis extinction during the lower power laser irradiation (Fig. S33a). The photothermal conversion efficiency of **Morp-TTDT$_2$** nanoparticles was calculated to be about 47.0 ± 1.0 % (mean ± SEM) according to the heating and cooling curves shown in Figure S34.

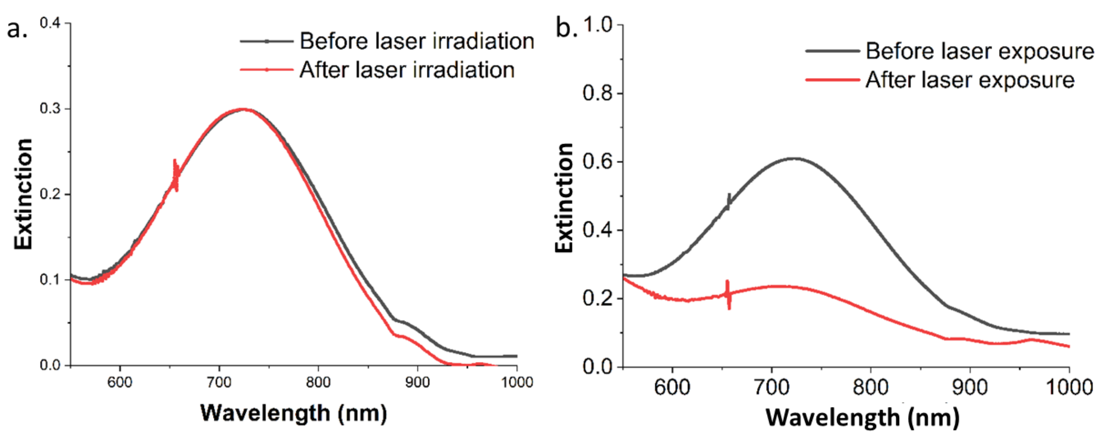

Figure S33: UV-Vis extinction curves for **Morp-TTDT$_2$** before and after laser irradiation (0.4 W/cm^2) (a) and UV-Vis extinction curves before and after laser irradiation (1.6 W/cm^2) (b)

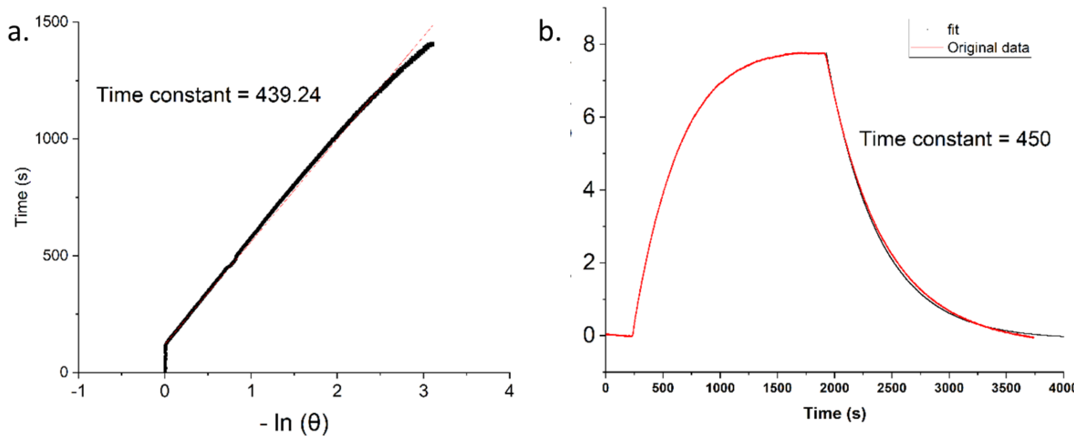

Figure S34: Linearized time data versus -ln (θ) for **Morp-TTDT₂** obtained from cooling period, fit to a best fit line (a) and non-linear least squares fitting of a single exponential decay to the time data obtained from the cooling period (b)

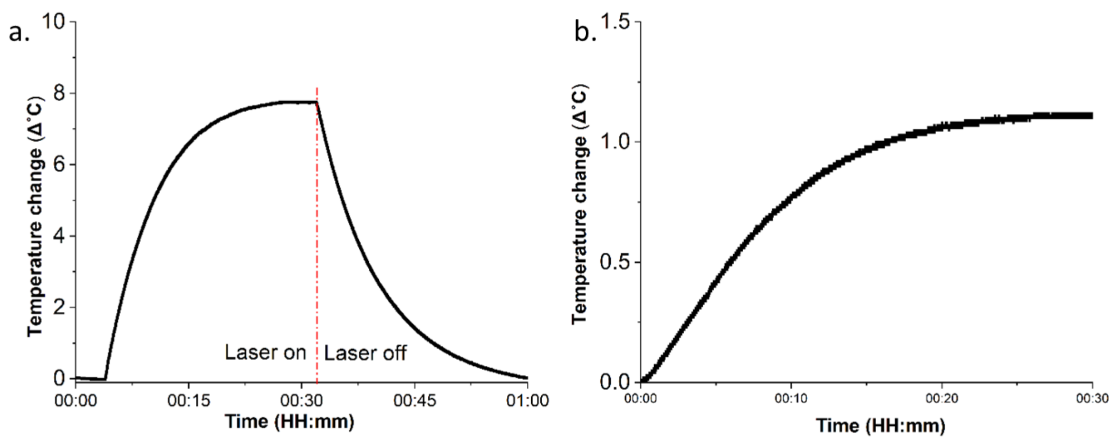

Figure S35: Photothermal effect of the irradiation of the **Morp-TTDT₂** nanoparticles with the NIR laser (808 nm, 0.4 W/cm^2), in which the irradiation lasted for 32 minutes, and then the laser was shut off (a) and Photothermal effect of the irradiation of solvent (water) with the NIR laser (808 nm, 0.4 W/cm^2) (b)

Photothermal properties of **Pip-TTDT₂** nanoparticles:

First, we used both linearized and non-linearized time data plots to calculate the time constants and selected 560 s as the time constant from the best fit (Fig. S36a). Photothermal conversion efficiency of **PIP-TTDT₂** nanoparticles was calculated to be about 46 ± 2 % (mean ± SEM) according to the heating and cooling curves shown in Figures S37.

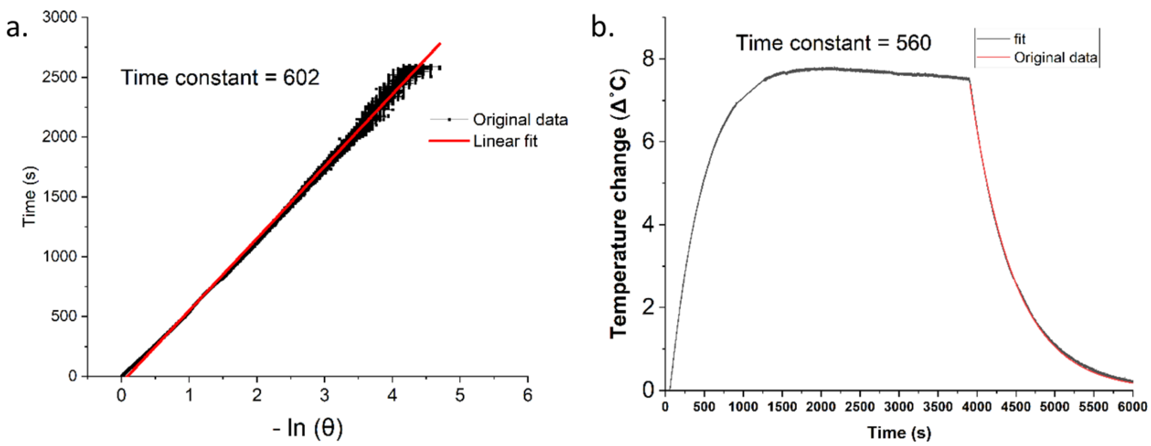

Figure S36: Linearized time data versus -ln (θ) for **Pip-TTDT$_2$** obtained from cooling period, fit to a best fit line (a) and Non-linear least squares fitting of a single exponential decay to the time data obtained from the cooling period (b)

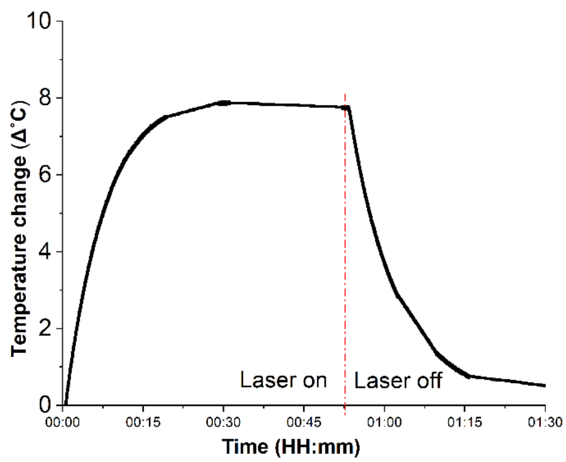

Figure S37: Photothermal effect of the irradiation of the **Pip-TTDT$_2$** nanoparticles with the NIR laser (808 nm, 0.4 W/cm^2), in which the irradiation lasted for 53 minutes, and then the laser was shut off.

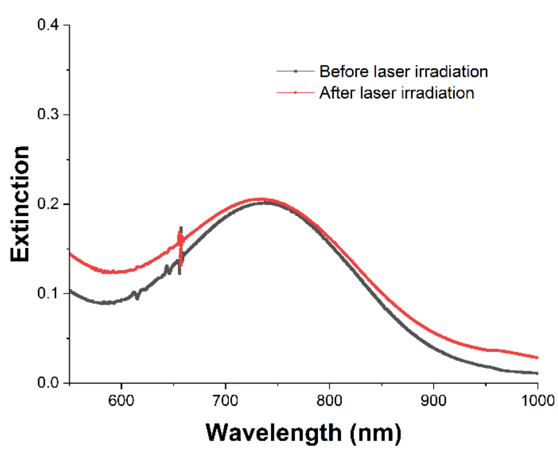

Figure S38: UV-Vis extinction curves before and after laser irradiation (0.4 W/cm^2) for **Pip-TTDT$_2$.**

Photothermal properties of **DMA-TTDT$_2$** nanoparticles:

Here, we used both linearized and non-linearized time data plots to calculate the time constants and selected 480 s as the time constant from the best fit (Fig. S39). Photothermal conversion efficiency of **DMA-TTDT$_2$** nanoparticles was calculated to be about 62.0 ± 3.5 % according to the heating and cooling curves shown in Figures S40.

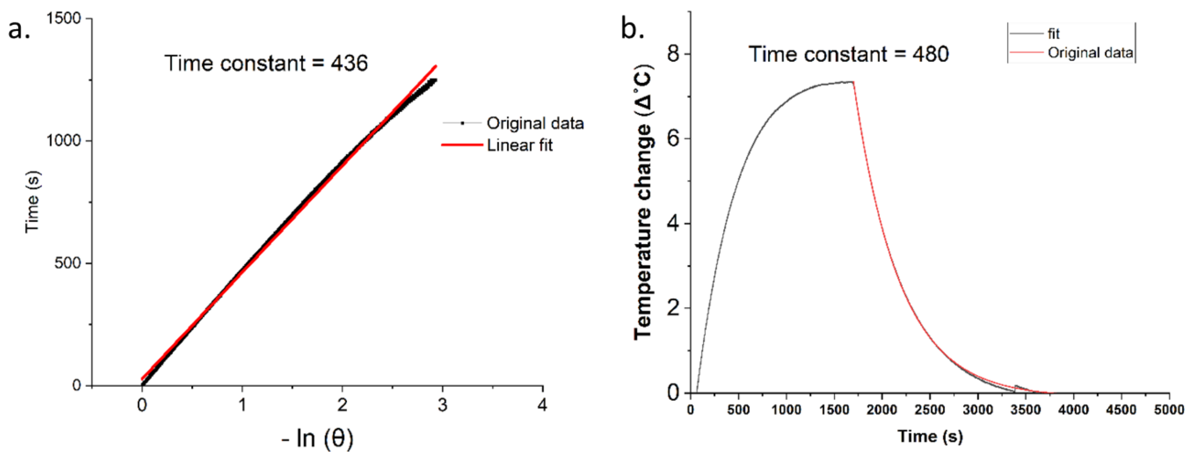

Figure S39: Linearized time data versus -ln (θ) for **DMA-TTDT$_2$** obtained from cooling period, fit to a best fit line (a) and Non-linear least squares fitting of a single exponential decay to the time data obtained from the cooling period (b)

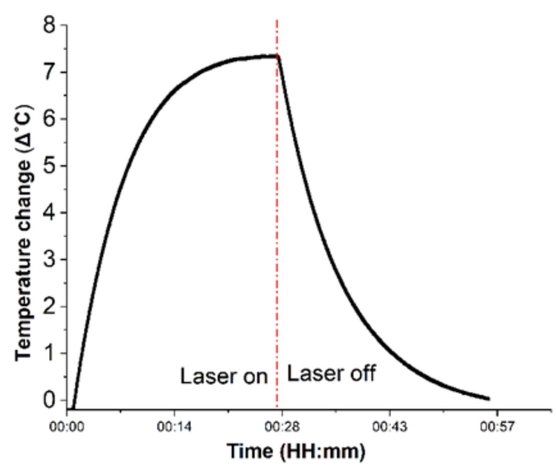

Figure S40: Photothermal effect of the irradiation of the **DMA-TTDT$_2$** nanoparticles with the NIR laser (808 nm, 0.4 W/cm^2), in which the irradiation lasted for 27 minutes, and then the laser was shut off

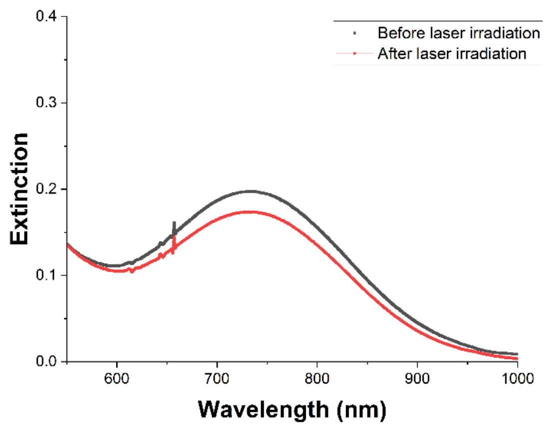

Figure S41: UV-Vis extinction curves before and after laser irradiation (0.4 W/cm^2) for **DMA-TTDT$_2$.**

Computational Assessment:

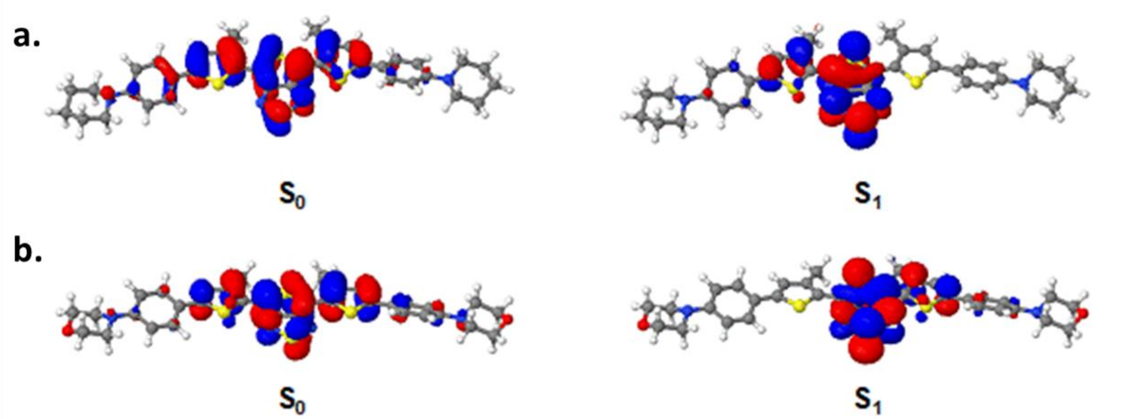

Figure S42: Ground (S_0) and excited (S_1) state natural transition orbitals (NTOs) for **Pip-TTDT$_2$** (a) and **Morp-TTDT$_2$** (b). The corresponding oscillator strengths for molecules (a) and (b) are 0.62 and 0.61, respectively. NTOs were computed using CAM-B3LYP with the cc-pVDZ basis set for the hydrogens and carbon atoms and aug-cc-pVDZ for the remaining elements.

Table S3: Ground (S_0) and excited (S_1) state dihedral angles (deg.) of the TTDT$_2$ derivatives computed using the CAM-B3LYP functional with the cc-pVDZ basis set for the hydrogens and carbon atoms and aug-cc-pVDZ for the remaining elements.

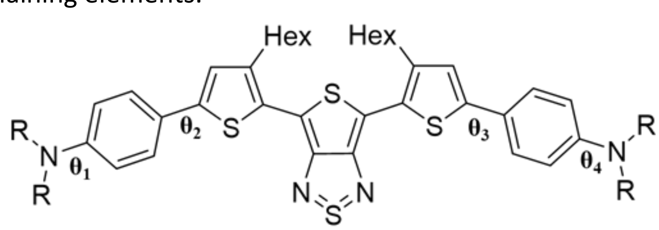

	θ_1	θ_2	θ_3	θ_4
	$S_0(S_1)$	**$S_0(S_1)$**	**$S_0(S_1)$**	**$S_0(S_1)$**
DMA-TTDT$_2$	9.0(3.5)	22.8(1.0)	22.9(1.1)	9.0(3.6)
Pip-TTDT$_2$	9.5(8.3)	24.2(9.8)	23.4(9.2)	9.6(8.7)
Morp-TTDT$_2$	4.8(3.0)	24.2(11.4)	23.9(11.3)	4.8(3.0)

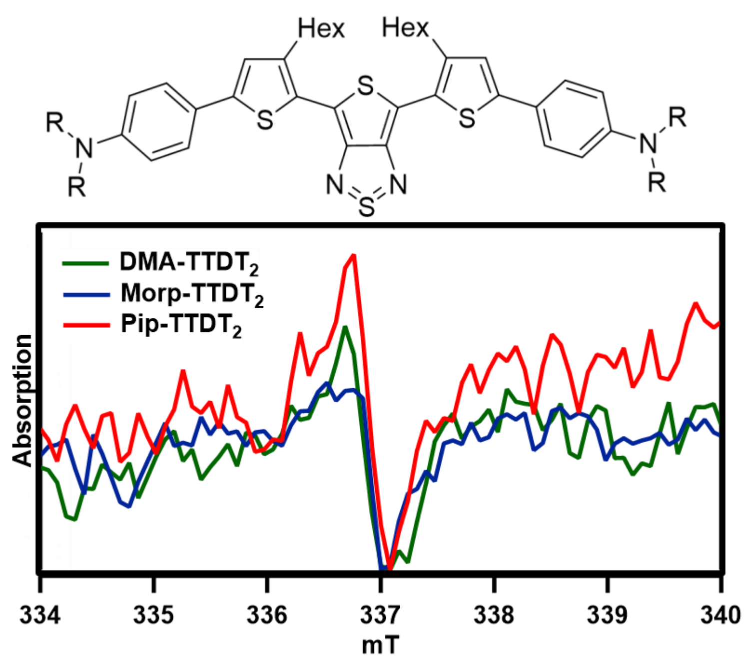

Figure S43: EPR spectra of the TTDT$_2$ derivatives in 1 mM $CDCl_3$

Table S4: Natural atomic charges of nitrogen atoms computed at the CAM-B3LYP level of theory with the cc-pVDZ basis set for the hydrogens and carbon atoms and aug-cc-pVDZ for the remaining elements. N-1 and N-4 denote the nitrogens on the donor groups, where N-2 and N-3 denote nitrogens on the acceptor group (as read from left to right).

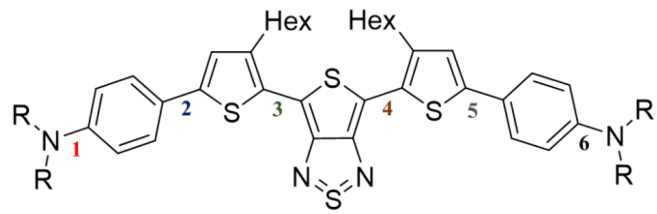

	Nitrogen Charge Density			
	N-1	**N-2**	**N-3**	**N-4**
DMA-TTDT$_2$	-0.5497	-0.6776	-0.6776	-0.5497
Pip-TTDT$_2$	-0.5970	-0.6772	-0.6773	-0.5972
Morp-TTDT$_2$	-0.5963	-0.6774	-0.6774	-0.5962

Table S5: Selected ground (S_0) and excited (S_1) state bond lengths (Å) of the $TTDT_2$ derivatives computed at the CAM-B3LYP level of theory with the cc-pVDZ basis set for the hydrogens and carbon atoms and aug-cc-pVDZ for the remaining elements.

Å	**1** **S_0 (S_1)**	**2** **S_0 (S_1)**	**3** **S_0 (S_1)**	**4** **S_0 (S_1)**	**5** **S_0 (S_1)**	**6** **S_0 (S_1)**
DMA-TTDT$_2$	1.382 (1.375)	1.465 (1.454)	1.429 (1.418)	1.429 (1.418)	1.465 (1.454)	1.382 (1.375)

Pip-$TTDT_2$	1.405 (1.398)	1.465 (1.455)	1.430 (1.142)	1.430 (1.418)	1.465 (1.455)	1.405 (1.399)
Morp-$TTDT_2$	1.404 (1.399)	1.465 (1.455)	1.430 (1.418)	1.430 (1.418)	1.465 (1.455)	1.404 (1.399)

Table S6: Theoretical (CAM-B3LYP) calculations of absorption/emission and the corresponding Stokes shifts along with the oscillator strength indicative of the most probable transition for the $TTDT_2$ derivatives.

	Absorbance	**Emission**	**Stokes Shift**	**Oscillator Strength**
	[nm (eV)]	**[nm (eV)]**	**[nm ($cm^{-1}x10^5$)]**	**S_0 (S_1)**
DMA-$TTDT_2$	763 (1.62)	843 (1.47)	79.2 (1.26)	0.620 (0.543)
Pip-$TTDT_2$	744 (1.67)	816 (1.52)	72.6 (1.38)	0.617 (0.537)
Morp-$TTDT_2$	740 (1.67)	811 (1.53)	70.5 (1.38)	0.611 (0.527)

Cartesian coordinates of molecules in S_0 and S_1 states:

1) S_0 geometry of DMA-$TTDT_2$:

```
C      -0.1841283309    3.4254790922    2.6407572170
C       0.1841564465    3.4849392740   -2.5615874377
C      -1.2947559365   -0.1572540651   11.6200211271
C      -0.3369999195   -2.3611092511   10.9860010594
C       1.2787950276    0.1111285897  -11.6231718043
C       0.3347701719   -2.1114772301  -11.0357078239
C      -0.1495708175   -1.0684020127    6.9730457940
C      -1.0891581172    1.0405912472    7.5785743453
C       0.1542399929   -0.9103235529   -6.9940638208
C       1.0811153989    1.2165642420   -7.5550557992
C      -0.2591959450   -1.5038702659    8.2840161730
C      -1.2006625479    0.6229095689    8.8945337107
```

C	0.2613046049	-1.3155144825	-8.3149221245
C	1.1899940311	0.8292690482	-8.8804787408
C	-0.3879775253	1.9709804046	4.7325232403
C	0.3876853634	2.0788269935	-4.6861573175
C	-0.2664642959	2.0945780317	3.3270222639
C	0.2696132657	2.1701584944	-3.2778962132
C	-0.5602072551	0.2119244726	6.5795835477
C	0.5600121516	0.3628255526	-6.5731956580
C	-0.7984733327	-0.6712921895	9.2855000902
C	0.7929692263	-0.4578382431	-9.2991503227
C	-0.4383568076	0.6780868228	5.1965100092
C	0.4411112257	0.7969741258	-5.1794863623
C	-0.0504514748	-0.7524980850	0.7131494263
C	0.0703187548	-0.7360720065	-0.7285423420
C	-0.2222215067	0.8542101608	2.6925714915
C	0.2312211826	0.9155899355	-2.6715936705
C	-0.1021733038	0.5320973186	1.3056952095
C	0.1141481290	0.5617370774	-1.2922244670
N	-0.9324548049	-1.1049160060	10.5910090521
N	0.9247558943	-0.8612293234	-10.6145417542
S	-0.3453140251	-0.4439995894	3.8694668033
S	0.3579096868	-0.3551504423	-3.8777546068
S	0.0021619738	1.7142320191	0.0197409477
H	-0.2242808573	4.2392829518	3.3771572379
H	-1.0140698527	3.5748440387	1.9319471628
H	0.7509397932	3.5370212119	2.0694024646
H	0.2219584010	4.3153107680	-3.2793843494
H	1.0139831633	3.6203121380	-1.8498555776
H	-0.7509819769	3.5811496334	-1.9875485489
H	-1.3617215990	-0.6796841220	12.5817881148
H	-2.2798646618	0.2941112131	11.4209762585
H	-0.5624421653	0.6661543271	11.7250331726
H	-0.5624346158	-2.5490538674	12.0425712110
H	0.7626101880	-2.3757602874	10.8596647169
H	-0.7519049568	-3.2005859891	10.4058207331
H	1.3462060943	-0.3894438178	-12.5964601020
H	2.2618148258	0.5637092317	-11.4166740937
H	0.5414863036	0.9324029475	-11.7081166422
H	0.5587938255	-2.2751489964	-12.0966167921
H	-0.7644702831	-2.1345567458	-10.9073443195
H	0.7552541064	-2.9612704101	-10.4749032013
H	0.2888276674	-1.7439924965	6.2358173631
H	-1.4401636806	2.0403835438	7.3182724325
H	-0.2781548219	-1.6045569524	-6.2707435232
H	1.4280439594	2.2120041911	-7.2735019576
H	0.0879838170	-2.5057834404	8.5274739081
H	-1.6198142933	1.3133637814	9.6235919054
H	-0.0819555469	-2.3133216921	-8.5798239815
H	1.6030559936	1.5380519899	-9.5952603884

H	-0.4094759982	2.8380356491	5.3922282640
H	0.4039191523	2.9607205323	-5.3260263969
N	-0.0925441407	-1.9746487928	1.2394982501
N	0.1197699739	-1.9459192933	-1.2819832323
S	0.0172626169	-3.0181579100	-0.0329774191

2) S_1 geometry of DMA-TTDT$_2$:

C	-0.2322176449	3.5050862007	2.6528217790
C	0.1915205559	3.5642938007	-2.5755454064
C	-0.8745472205	-0.1804703696	11.6211474581
C	-0.8427301168	-2.5459826624	10.8165892096
C	0.9153729097	0.0865156327	-11.6191798292
C	0.8311832587	-2.2969888436	-10.8736165688
C	-0.5791179216	-1.1341655055	6.8494850447
C	-0.6085857903	1.1289466304	7.6201395730
C	0.5546204865	-0.9782109167	-6.8755178736
C	0.6377140596	1.3021451430	-7.5894608615
C	-0.6850449364	-1.5888245520	8.1508531995
C	-0.7148497093	0.6916034710	8.9267962632
C	0.6642814602	-1.4027022737	-8.1867438923
C	0.7477536800	0.8951136977	-8.9055487373
C	-0.3951183932	2.0198875371	4.7137280014
C	0.3741954329	2.1262223428	-4.6679544681
C	-0.2804087287	2.1643104054	3.3221271567
C	0.2584698339	2.2390444742	-3.2735278262
C	-0.5381741692	0.2356898795	6.5361165307
C	0.5381362183	0.3840707306	-6.5287033069
C	-0.7616253474	-0.6867788136	9.2343694972
C	0.7695913706	-0.4759564268	-9.2467725690
C	-0.4264221154	0.7118704181	5.1671727996
C	0.4219491350	0.8288228094	-5.1495881833
C	-0.0503297797	-0.6755487468	0.7100841263
C	0.0665130875	-0.6593360700	-0.7234592552
C	-0.2199334651	0.9232346288	2.6651996583
C	0.2146445462	0.9833917492	-2.6435465477
C	-0.1048400034	0.6146360930	1.2858551170
C	0.1038827945	0.6435826326	-1.2712159061
N	-0.8766594610	-1.1294232183	10.5314585476
N	0.8886072210	-0.8887258517	-10.5533115201
S	-0.3085120134	-0.3909760219	3.8256356625
S	0.3213832214	-0.3041879500	-3.8319838416
S	-0.0086407683	1.8234704806	0.0201710131
H	-0.2977390892	4.3068899611	3.4005114300
H	-1.0627040181	3.6397784163	1.9423478097
H	0.7018242450	3.6487535616	2.0875177715
H	0.2452452638	4.3828339660	-3.3058424453

H	1.0204144917	3.6954952676	-1.8625589234
H	-0.7441460930	3.6824800836	-2.0070500533
H	-0.9852359171	-0.7198412500	12.5688701647
H	-1.7116862899	0.5336073536	11.5422856934
H	0.0620815469	0.4044200740	11.6683297605
H	-0.9573201824	-2.6989591999	11.8958753226
H	0.1075637707	-3.0153014204	10.5035940942
H	-1.6636977760	-3.0833197951	10.3126103891
H	1.0236262705	-0.4315544112	-12.5789803494
H	1.7659358412	0.7813733498	-11.5157449302
H	-0.0088685678	0.6912415178	-11.6597815943
H	0.9530618729	-2.4255742976	-11.9552751012
H	-0.1305156729	-2.7559969502	-10.5808343968
H	1.6372914208	-2.8617218599	-10.3756455075
H	-0.5256108755	-1.8737689658	6.0484150839
H	-0.5757813749	2.2036900839	7.4391314642
H	0.4761934536	-1.7360431590	-6.0937715187
H	0.6283519680	2.3725110639	-7.3817708711
H	-0.7091288487	-2.6624839201	8.3248607414
H	-0.7614950287	1.4341846994	9.7206981044
H	0.6677449070	-2.4720163086	-8.3871589448
H	0.8187022189	1.6559469797	-9.6801291241
H	-0.4565224754	2.8809774555	5.3778800604
H	0.4203309861	3.0021822823	-5.3136448586
N	-0.0878731512	-1.8870703099	1.2587082507
N	0.1204225910	-1.8581592442	-1.2980089770
S	0.0228198387	-2.9510864982	-0.0312986767

3) S_0 geometry of Pip-TTDT$_2$:

C	0.5084049222	1.2891207009	4.2812560932
C	1.0466558304	2.2180424159	3.2342912573
C	1.7122195457	3.4254083520	3.5591939636
C	2.1517778100	4.1505204660	2.4778986176
C	2.8751314797	5.4248254956	2.4722707711
C	2.7982593451	6.3026346200	3.5664209293
C	3.4840040973	7.5032314960	3.5787667969
C	4.2905297680	7.8983596411	2.4949022127
N	4.9493063731	9.1386707936	2.5257797614
C	5.5594166992	9.6143586278	1.2939401999
C	5.8319002168	11.1142470698	1.3663563638
C	6.6822158086	11.4696280198	2.5818913892
C	6.0359270045	10.9147680576	3.8476902297
C	5.7675089429	9.4220852525	3.7049089650
C	4.3653981970	7.0252762164	1.4002335440
C	3.6693526606	5.8217692956	1.3925783851
S	1.7306607235	3.3433387223	0.9956039541

C	0.9744027319	2.0132854711	1.8574354469
C	0.4011970830	0.9349353854	1.1143183250
C	0.3614837367	0.7735914007	-0.2913121843
C	-0.2935365977	-0.4389272943	-0.7304511441
N	-0.3269925376	-0.5877402526	-2.0533621020
S	0.4289469725	0.7382803339	-2.6763338550
N	0.8175911980	1.5332283223	-1.2853476420
C	-0.7800771611	-1.2493854187	0.3229950012
C	-1.4615964576	-2.5021171638	0.2230047184
C	-1.9667407045	-3.3330308545	1.2216303398
C	-1.9036969447	-3.0599755444	2.6948024650
C	-2.5768218834	-4.4953736341	0.6895771017
C	-2.5563254200	-4.5809399506	-0.6816805577
C	-3.0966849328	-5.6437511574	-1.5335435755
C	-3.2763805900	-6.9447507365	-1.0349231640
C	-3.7878088530	-7.9571796812	-1.8256976763
C	-4.1519616039	-7.7276175039	-3.1658710737
N	-4.6343058464	-8.7859010515	-3.9534263662
C	-4.7567549632	-8.5665539073	-5.3861289657
C	-4.8517771921	-9.8944763215	-6.1327725674
C	-5.9943137606	-10.7540340389	-5.6011962017
C	-5.8574976988	-10.9225735216	-4.0909750623
C	-5.7443779807	-9.5661511339	-3.4068843460
C	-3.9734126873	-6.4294881819	-3.6653000226
C	-3.4534563947	-5.4175976472	-2.8660481975
S	-1.7526540917	-3.1969561324	-1.3632636480
S	-0.3927195912	-0.4496824605	1.8293038063
H	0.7075382195	1.6870972834	5.2852615206
H	0.9675620191	0.2897413172	4.2205128056
H	-0.5802256463	1.1498000505	4.1868078516
H	1.8867869075	3.7343869424	4.5895012469
H	2.1576751658	6.0524516680	4.4134109565
H	3.3623834181	8.1739587394	4.4295872627
H	4.8726954580	9.4086437016	0.4622108382
H	6.5081738408	9.0746747199	1.0780236590
H	4.8658319239	11.6427610482	1.4252860227
H	6.3238862710	11.4359586638	0.4352260701
H	6.8176974598	12.5596592772	2.6566676714
H	7.6897880789	11.0317478075	2.4653374329
H	5.0798881277	11.4320116277	4.0344208696
H	6.6795502426	11.0855905140	4.7248713155
H	5.2585302445	9.0423573781	4.5978275461
H	6.7356972452	8.8793544978	3.6326363231
H	4.9905311532	7.2676295049	0.5427413856
H	3.7744693282	5.1624744827	0.5287137766
H	-2.4041175805	-2.1153644913	2.9602570158
H	-0.8653847379	-2.9868962736	3.0555194031
H	-2.3948951185	-3.8666896140	3.2551448107
H	-3.0508042366	-5.2455384003	1.3221435891

H	-2.9737014285	-7.1756029113	-0.0124616048
H	-3.8693755979	-8.9625167654	-1.4119608505
H	-3.8716372820	-8.0167764234	-5.7323310931
H	-5.6461033869	-7.9419925545	-5.6246214834
H	-3.8976798345	-10.4335088152	-6.0096510747
H	-4.9778220038	-9.6946085137	-7.2082756322
H	-6.0111794661	-11.7330027094	-6.1046456234
H	-6.9582861531	-10.2640113087	-5.8273986046
H	-4.9536605894	-11.5121461852	-3.8633442360
H	-6.7198793820	-11.4677813300	-3.6763807263
H	-5.5982633949	-9.6968292005	-2.3288806443
H	-6.6980591598	-9.0086165961	-3.5362472572
H	-4.2600745612	-6.1876292231	-4.6871021512
H	-3.3502349715	-4.4167385873	-3.2898574356

4) S_1 geometry of Pip-TTDT$_2$:

C	0.5178676810	1.2673601272	4.3649525765
C	1.0567658566	2.1791161879	3.3038729908
C	1.7209107873	3.3787223807	3.6055711725
C	2.1600251849	4.0968254318	2.5066655320
C	2.8781600903	5.3620598215	2.4884768487
C	3.0490311633	6.1214631970	3.6625638057
C	3.7301324872	7.3217537433	3.6570339077
C	4.2901793730	7.8454409130	2.4733630766
N	4.9462395400	9.0804556096	2.4903084653
C	5.3048303277	9.6927899809	1.2199390076
C	5.5415857718	11.1916256965	1.3857426970
C	6.5841142823	11.4797573122	2.4611443011
C	6.1898120962	10.7898373444	3.7633953684
C	5.9481495931	9.3037434826	3.5323762649
C	4.1219477315	7.0911265989	1.2999443913
C	3.4315299590	5.8880139594	1.3119431942
S	1.7358674679	3.2688472091	1.0366379530
C	0.9757065054	1.9553050047	1.9183735357
C	0.3995695454	0.8831097717	1.1905269839
C	0.3730254489	0.7344719844	-0.2155057910
C	-0.2817357614	-0.4691353335	-0.6521714956
N	-0.3212602544	-0.6423251208	-1.9704213579
S	0.4551144273	0.6987585036	-2.6078935712
N	0.8445285294	1.5051749141	-1.1916942123
C	-0.7713597313	-1.2618605088	0.4115582736
C	-1.4570257161	-2.4983306993	0.3007687219
C	-1.9849025990	-3.3421963572	1.2935825538
C	-1.9342999786	-3.0854688068	2.7697721623
C	-2.5911106901	-4.4841874191	0.7463396539
C	-2.5559806119	-4.5600589321	-0.6353967823

C	-3.0935302159	-5.6059176625	-1.4920226942
C	-3.5662464307	-6.8190278532	-0.9543455510
C	-4.0761848316	-7.8186792661	-1.7577097938
C	-4.1501678534	-7.6722635429	-3.1585014538
N	-4.6372824280	-8.7152542481	-3.9525368724
C	-4.4873688422	-8.6150680299	-5.3964664880
C	-4.6023911211	-9.9880961485	-6.0535176791
C	-5.9025981061	-10.6874406941	-5.6707576077
C	-6.0340826568	-10.7398400029	-4.1517568131
C	-5.8948132294	-9.3463945482	-3.5526021630
C	-3.6814783906	-6.4626518005	-3.6986521661
C	-3.1649369254	-5.4645553682	-2.8855715115
S	-1.7390405091	-3.1729188502	-1.2948760579
S	-0.4000067847	-0.4853871938	1.9380427024
H	0.7207094819	1.6811126688	5.3618281756
H	0.9743382373	0.2663861163	4.3175593932
H	-0.5709711147	1.1301705122	4.2740679982
H	1.8884269049	3.7028429335	4.6318979619
H	2.6135146919	5.7749102337	4.6001976487
H	3.7996199539	7.8913460597	4.5835809887
H	4.4834565927	9.5325430168	0.5098643488
H	6.2121969274	9.2171416262	0.7873409787
H	4.5862838820	11.6679337108	1.6626164436
H	5.8485921954	11.6153471762	0.4169483140
H	6.6974941312	12.5643941588	2.6114698286
H	7.5677418555	11.1006671801	2.1305166131
H	5.2662080536	11.2437103143	4.1600705294
H	6.9727466974	10.9149419906	4.5276305082
H	5.6197178124	8.8247181710	4.4609039281
H	6.9043165246	8.8166655146	3.2416012242
H	4.5526278893	7.4305327636	0.3598663756
H	3.3430614761	5.3321739101	0.3766240412
H	-2.4343684157	-2.1424553727	3.0401925266
H	-0.8992494583	-3.0195352058	3.1399923855
H	-2.4332853679	-3.8976979733	3.3150883646
H	-3.0667170885	-5.2398917493	1.3702427090
H	-3.5069300119	-6.9947778513	0.1201617764
H	-4.3897581681	-8.7547716604	-1.2961971893
H	-3.4994395339	-8.1911388903	-5.6172839153
H	-5.2457150074	-7.9279056753	-5.8315777906
H	-3.7456382748	-10.6029988705	-5.7309903493
H	-4.5259727647	-9.8699051533	-7.1455550419
H	-5.9411264628	-11.6992964534	-6.1026368834
H	-6.7582091789	-10.1295599620	-6.0916773998
H	-5.2471925242	-11.3888430395	-3.7323140819
H	-7.0052453636	-11.1658617232	-3.8551261358
H	-5.9441569831	-9.3978038161	-2.4597438033
H	-6.7500518264	-8.7174747764	-3.8826367912

H	-3.7359402129	-6.2794441006	-4.7699992178
H	-2.8286779048	-4.5374246828	-3.3535372988

5) S_0 geometry of Morp-TTDT$_2$:

C	0.1946318026	1.4030429529	4.2724860105
C	0.7662015645	2.3259456159	3.2379156957
C	1.3521895734	3.5718130816	3.5706417957
C	1.8367551947	4.2847010955	2.5006511365
C	2.4970906814	5.5928604910	2.5055155918
C	2.2896584066	6.5007515627	3.5566270390
C	2.9111243812	7.7360106992	3.5791542635
C	3.7785203465	8.1375965319	2.5465438571
N	4.3658015440	9.4128541486	2.5731755422
C	5.1326198447	9.8372808895	1.4134331945
C	5.3830546102	11.3361251872	1.4816317154
O	6.0336551707	11.7039787505	2.6783022881
C	5.2527620228	11.3335011362	3.7939325852
C	5.0021026942	9.8359096706	3.8186874627
C	3.9871658538	7.2331050102	1.4955625979
C	3.3558175498	5.9948200732	1.4782591519
S	1.5627365504	3.4159487161	1.0188978574
C	0.8038183099	2.0788317373	1.8669420383
C	0.3316056477	0.9552940300	1.1194242277
C	0.4090002418	0.7477089636	-0.2783391894
C	-0.1695649778	-0.5004381416	-0.7245316711
N	-0.0938356909	-0.6931423386	-2.0400988301
S	0.6667059849	0.6370799811	-2.6470292784
N	0.9169426065	1.4909672957	-1.2597244204
C	-0.7121957532	-1.2921023187	0.3154799843
C	-1.3455656625	-2.5692470616	0.2065046266
C	-1.9045672800	-3.3819086317	1.1909510956
C	-1.9678163901	-3.0574660818	2.6536689823
C	-2.4354998182	-4.5802621120	0.6539191362
C	-2.3020681073	-4.7102926286	-0.7073979025
C	-2.7423622472	-5.8168095806	-1.5613203543
C	-2.9255410638	-7.1052022980	-1.0334377223
C	-3.3464329717	-8.1583707876	-1.8248980288
C	-3.6082576487	-7.9838704775	-3.1963197563
N	-3.9961729977	-9.0780984408	-3.9865365652
C	-4.1101422269	-8.8782214061	-5.4218491108
C	-4.1953832562	-10.2243709981	-6.1250012265
O	-5.2667744360	-11.0023794478	-5.6377166831
C	-5.1142974616	-11.2331536658	-4.2538315967
C	-5.0707722538	-9.9280477404	-3.4784931533
C	-3.4264152481	-6.6982457541	-3.7259180420
C	-2.9991732191	-5.6457217784	-2.9247193807

S	-1.4877409536	-3.3245761832	-1.3721752929
S	-0.4696293637	-0.4324690941	1.8183319598
H	0.3140768058	1.8318296674	5.2764300553
H	0.6917557008	0.4201724550	4.2670969907
H	-0.8800739690	1.2213493168	4.1125895133
H	1.4369577955	3.9185712623	4.6002694572
H	1.5982128317	6.2443463486	4.3606019716
H	2.6885160897	8.4222698833	4.3960220174
H	4.5631109618	9.6162403847	0.5000004124
H	6.1054590123	9.3061335144	1.3481790571
H	4.4166807609	11.8709090799	1.3946699598
H	6.0349183638	11.6506375664	0.6551374033
H	4.2828236741	11.8689901870	3.7747697131
H	5.8096138913	11.6428400060	4.6892079173
H	4.3603170682	9.5922390498	4.6735987716
H	5.9681842580	9.3083049956	3.9598440591
H	4.6658316189	7.4792757975	0.6811268093
H	3.5631611238	5.3139114971	0.6504715483
H	-2.5154443898	-2.1210002985	2.8442550979
H	-0.9642659306	-2.9387242967	3.0922416992
H	-2.4783005045	-3.8600894335	3.2025001713
H	-2.9368420861	-5.3236673041	1.2732572555
H	-2.7007724884	-7.2931523608	0.0174517215
H	-3.4361584067	-9.1486971899	-1.3788196981
H	-3.2207187813	-8.3459766379	-5.7867819079
H	-5.0033789939	-8.2721008654	-5.6817560164
H	-3.2391457110	-10.7671926120	-5.9892648877
H	-4.3690823586	-10.0811998479	-7.2003024630
H	-4.1850083128	-11.8058394150	-4.0632090151
H	-5.9741430375	-11.8386268657	-3.9354448011
H	-4.9111346471	-10.1457559034	-2.4158009887
H	-6.0501005414	-9.4151647821	-3.5753990962
H	-3.6365753932	-6.4976184885	-4.7747204545
H	-2.8902150528	-4.6569797405	-3.3745702337

6) S_1 geometry of Morp-TTDT$_2$:

C	0.1581262629	1.4101641066	4.3614757249
C	0.7298020255	2.3136705095	3.3105694685
C	1.3144258844	3.5529878480	3.6169577814
C	1.8009487341	4.2549029586	2.5278451424
C	2.4626374163	5.5510045976	2.5164254516
C	2.4775396021	6.3736256633	3.6588825890
C	3.1065303372	7.6026984211	3.6609245124
C	3.7646518091	8.0936272732	2.5150241348
N	4.3636571473	9.3574486264	2.5253355265
C	4.9370417481	9.8625244431	1.2877894623
C	5.1915140121	11.3578071012	1.4044067101
O	6.0122676221	11.6657823940	2.5092647502

C	5.4034215264	11.2297479019	3.7047676663
C	5.1669585686	9.7297731139	3.6878005224
C	3.7534699584	7.2752713925	1.3727549190
C	3.1155140923	6.0438774534	1.3773575334
S	1.5238544422	3.3622565456	1.0611407633
C	0.7612057247	2.0424248089	1.9314530189
C	0.2886011609	0.9222489760	1.2014980529
C	0.3718640296	0.7304267493	-0.1969549895
C	-0.1973602589	-0.5136679725	-0.6394283387
N	-0.1335315960	-0.7275144144	-1.9506699009
S	0.6295473230	0.6272214845	-2.5746606492
N	0.8798876691	1.4921406479	-1.1617511076
C	-0.7288867494	-1.2955804631	0.4120055418
C	-1.3512330043	-2.5641156512	0.2916693420
C	-1.9095207688	-3.4045673235	1.2707050003
C	-1.9722015798	-3.1068427920	2.7386902564
C	-2.4267780493	-4.5867435173	0.7170851793
C	-2.2935246100	-4.6961235265	-0.6562171313
C	-2.7281912796	-5.7851799190	-1.5180803171
C	-3.1573164207	-7.0143653695	-0.9823239246
C	-3.5735426212	-8.0535648194	-1.7905374141
C	-3.5875224897	-7.9323740767	-3.1949339245
N	-3.9750577937	-9.0095213047	-3.9984843162
C	-3.8715492759	-8.8688813602	-5.4423414664
C	-3.9736831756	-10.2333737679	-6.1068088987
O	-5.1595575144	-10.9055382807	-5.7445364002
C	-5.2048065032	-11.0939904535	-4.3472157348
C	-5.1627637551	-9.7669147499	-3.6099149484
C	-3.1626547220	-6.7062104683	-3.7339600106
C	-2.7417337496	-5.6687575958	-2.9155757958
S	-1.4924962817	-3.2925282268	-1.2990111579
S	-0.5039619876	-0.4580883400	1.9350310516
H	0.2769335769	1.8598834526	5.3562928720
H	0.6566170978	0.4284410124	4.3750140311
H	-0.9158413006	1.2247002941	4.2034317664
H	1.3935251080	3.9167456526	4.6407282516
H	1.9607982570	6.0525109747	4.5637755676
H	3.0562665295	8.2128398596	4.5619692584
H	4.2311225171	9.6925475123	0.4635078168
H	5.8866146729	9.3449194019	1.0387156897
H	4.2221130501	11.8870330206	1.4923743172
H	5.7112777031	11.7237452143	0.5084925062
H	4.4387129720	11.7540202521	3.8544703966
H	6.0824248753	11.4987630015	4.5255558982
H	4.6561597481	9.4376783866	4.6124095984
H	6.1454845766	9.2078281159	3.6627757360
H	4.2655424694	7.5863486267	0.4645306654
H	3.1503381591	5.4392274029	0.4692561804
H	-2.5332103244	-2.1824828337	2.9468941258

H	-0.9690956868	-2.9808780776	3.1752958847
H	-2.4688482649	-3.9276782792	3.2730861033
H	-2.9130428484	-5.3460436402	1.3283857458
H	-3.1409269725	-7.1696833413	0.0968471189
H	-3.8613604742	-8.9946161887	-1.3233357851
H	-2.8972922303	-8.4297562815	-5.6964644671
H	-4.6634805923	-8.2031254961	-5.8439684811
H	-3.0914499119	-10.8424404868	-5.8270623569
H	-3.9909261042	-10.1214097884	-7.1994575428
H	-4.3547998897	-11.7252524424	-4.0202288352
H	-6.1423704411	-11.6225281631	-4.1264186668
H	-5.1560105536	-9.9577469640	-2.5306878731
H	-6.0809393207	-9.1908183487	-3.8457258991
H	-3.1750294540	-6.5410324183	-4.8093093843
H	-2.4368889472	-4.7309624312	-3.3836502432

References:

(1) Yanai, T.; Tew, D. P.; Handy, N. C. A New Hybrid Exchange–Correlation Functional Using the Coulomb-Attenuating Method (CAM-B3LYP). *Chem. Phys. Lett.* **2004**, *393* (1), 51–57. https://doi.org/10.1016/j.cplett.2004.06.011.

(2) Dunning, T. H. Gaussian Basis Sets for Use in Correlated Molecular Calculations. I. The Atoms Boron through Neon and Hydrogen. *J. Chem. Phys.* **1989**, *90* (2), 1007–1023. https://doi.org/10.1063/1.456153.

(3) Woon, D. E.; Dunning, T. H., Jr. Gaussian Basis Sets for Use in Correlated Molecular Calculations. III. The Atoms Aluminum through Argon. *J. Chem. Phys.* **1993**, *98* (2), 1358–1371. https://doi.org/10.1063/1.464303.

(4) Marques, M. A. L.; Gross, E. K. U. Time-Dependent Density Functional Theory. *Annu. Rev. Phys. Chem.* **2004**, *55* (1), 427–455. https://doi.org/10.1146/annurev.physchem.55.091602.094449.

(5) Kendall, R. A.; Dunning, T. H., Jr.; Harrison, R. J. Electron Affinities of the First-row Atoms Revisited. Systematic Basis Sets and Wave Functions. *J. Chem. Phys.* **1992**, *96* (9), 6796–6806. https://doi.org/10.1063/1.462569.

(6) Mennucci, B. Polarizable Continuum Model. *WIREs Comput. Mol. Sci.* **2012**, *2* (3), 386–404. https://doi.org/10.1002/wcms.1086.

(7) Martin, R. L. Natural Transition Orbitals. *J. Chem. Phys.* **2003**, *118* (11), 4775–4777. https://doi.org/10.1063/1.1558471.

(8) Glendening, E. D.; Landis, C. R.; Weinhold, F. Natural Bond Orbital Methods. *WIREs Comput. Mol. Sci.* **2012**, *2* (1), 1–42. https://doi.org/10.1002/wcms.51.

(9) *Ohio Supercomputer Center*. Ohio Supercomputer Center. https://www.osc.edu/ (accessed 2023-03-09).

(10) Epifanovsky, E.; Gilbert, A. T. B.; Feng, X.; Lee, J.; Mao, Y.; Mardirossian, N.; Pokhilko, P.; White, A. F.; Coons, M. P.; Dempwolff, A. L.; Gan, Z.; Hait, D.; Horn, P. R.; Jacobson, L. D.; Kaliman, I.; Kussmann, J.; Lange, A. W.; Lao, K. U.; Levine, D. S.; Liu, J.; McKenzie, S. C.; Morrison, A. F.; Nanda, K. D.; Plasser, F.; Rehn, D. R.; Vidal, M. L.; You, Z.-Q.; Zhu, Y.; Alam, B.; Albrecht, B. J.; Aldossary, A.; Alguire, E.; Andersen, J. H.; Athavale, V.; Barton, D.; Begam, K.; Behn, A.; Bellonzi, N.; Bernard, Y. A.; Berquist, E. J.; Burton, H. G. A.; Carreras, A.; Carter-Fenk, K.; Chakraborty, R.; Chien, A. D.; Closser, K. D.; Cofer-Shabica, V.; Dasgupta, S.; de Wergifosse, M.; Deng, J.; Diedenhofen, M.; Do, H.; Ehlert, S.; Fang, P.-T.; Fatehi, S.; Feng, Q.; Friedhoff, T.; Gayvert, J.; Ge, Q.; Gidofalvi, G.; Goldey, M.; Gomes, J.; González-Espinoza, C. E.; Gulania, S.; Gunina, A. O.; Hanson-Heine, M. W. D.;

Harbach, P. H. P.; Hauser, A.; Herbst, M. F.; Hernández Vera, M.; Hodecker, M.; Holden, Z. C.; Houck, S.; Huang, X.; Hui, K.; Huynh, B. C.; Ivanov, M.; Jász, Á.; Ji, H.; Jiang, H.; Kaduk, B.; Kähler, S.; Khistyaev, K.; Kim, J.; Kis, G.; Klunzinger, P.; Koczor-Benda, Z.; Koh, J. H.; Kosenkov, D.; Koulias, L.; Kowalczyk, T.; Krauter, C. M.; Kue, K.; Kunitsa, A.; Kus, T.; Ladjánszki, I.; Landau, A.; Lawler, K. V.; Lefrancois, D.; Lehtola, S.; Li, R. R.; Li, Y.-P.; Liang, J.; Liebenthal, M.; Lin, H.-H.; Lin, Y.-S.; Liu, F.; Liu, K.-Y.; Loipersberger, M.; Luenser, A.; Manjanath, A.; Manohar, P.; Mansoor, E.; Manzer, S. F.; Mao, S.-P.; Marenich, A. V.; Markovich, T.; Mason, S.; Maurer, S. A.; McLaughlin, P. F.; Menger, M. F. S. J.; Mewes, J.-M.; Mewes, S. A.; Morgante, P.; Mullinax, J. W.; Oosterbaan, K. J.; Paran, G.; Paul, A. C.; Paul, S. K.; Pavošević, F.; Pei, Z.; Prager, S.; Proynov, E. I.; Rák, Á.; Ramos-Cordoba, E.; Rana, B.; Rask, A. E.; Rettig, A.; Richard, R. M.; Rob, F.; Rossomme, E.; Scheele, T.; Scheurer, M.; Schneider, M.; Sergueev, N.; Sharada, S. M.; Skomorowski, W.; Small, D. W.; Stein, C. J.; Su, Y.-C.; Sundstrom, E. J.; Tao, Z.; Thirman, J.; Tornai, G. J.; Tsuchimochi, T.; Tubman, N. M.; Veccham, S. P.; Vydrov, O.; Wenzel, J.; Witte, J.; Yamada, A.; Yao, K.; Yeganeh, S.; Yost, S. R.; Zech, A.; Zhang, I. Y.; Zhang, X.; Zhang, Y.; Zuev, D.; Aspuru-Guzik, A.; Bell, A. T.; Besley, N. A.; Bravaya, K. B.; Brooks, B. R.; Casanova, D.; Chai, J.-D.; Coriani, S.; Cramer, C. J.; Cserey, G.; DePrince, A. E., III; DiStasio, R. A., Jr.; Dreuw, A.; Dunietz, B. D.; Furlani, T. R.; Goddard, W. A., III; Hammes-Schiffer, S.; Head-Gordon, T.; Hehre, W. J.; Hsu, C.-P.; Jagau, T.-C.; Jung, Y.; Klamt, A.; Kong, J.; Lambrecht, D. S.; Liang, W.; Mayhall, N. J.; McCurdy, C. W.; Neaton, J. B.; Ochsenfeld, C.; Parkhill, J. A.; Peverati, R.; Rassolov, V. A.; Shao, Y.; Slipchenko, L. V.; Stauch, T.; Steele, R. P.; Subotnik, J. E.; Thom, A. J. W.; Tkatchenko, A.; Truhlar, D. G.; Van Voorhis, T.; Wesolowski, T. A.; Whaley, K. B.; Woodcock, H. L., III; Zimmerman, P. M.; Faraji, S.; Gill, P. M. W.; Head-Gordon, M.; Herbert, J. M.; Krylov, A. I. Software for the Frontiers of Quantum Chemistry: An Overview of Developments in the Q-Chem 5 Package. *J. Chem. Phys.* **2021**, *155* (8), 084801. https://doi.org/10.1063/5.0055522.

(11) Zhang, Y.; Autry, S. A.; McNamara, L. E.; Nguyen, S. T.; Le, N.; Brogdon, P.; Watkins, D. L.; Hammer, N. I.; Delcamp, J. H. Near-Infrared Fluorescent Thienothiadiazole Dyes with Large Stokes Shifts and High Photostability. *J. Org. Chem.* **2017**, *82* (11), 5597–5606. https://doi.org/10.1021/acs.joc.7b00422.